associations. MeSH profiles illustrate the features of genes and diseases. Comparing profiles emphasizes the differences and similarities between the features of genes and diseases. Gendoo will accelerate the analysis of omics data from biological and clinical perspectives.

SUPPLEMENTARY DATA

Supplementary Data are available at NAR Online.

ACKNOWLEDGEMENTS

We thank Prof. Shoko Kawamoto and Prof. Kousaku Okubo for their helpful discussions.

FUNDING

Integrated Database Project of the Ministry of Education, Culture, Sports, Science and Technology of Japan. Funding for open access charge: Integrated Database Project.

Conflict of interest statement. None declared.

REFERENCES

1. Butte,A.J. and Kohane,I.S. (2006) Creation and implications of a phenome-genome network. *Nat. Biotechnol.*, **24**, 55–62.
2. Perez-Iratxeta,C., Wjst,M., Bork,P. and Andrade,M.A. (2005) G2D: a tool for mining genes associated with disease. *BMC Genet.*, **6**, 45.
3. Perez-Iratxeta,C., Bork,P. and Andrade,M.A. (2002) Association of genes to genetically inherited diseases using data mining. *Nat. Genet.*, **31**, 316–319.
4. Ashburner,M., Ball,C.A., Blake,J.A., Botstein,D., Butler,H., Cherry,J.M., Davis,A.P., Dolinski,K., Dwight,S.S., Eppig,J.T. *et al.* (2000) Gene ontology: tool for the unification of biology. The gene ontology consortium. *Nat. Genet.*, **25**, 25–29.
5. Maglott,D., Ostell,J., Pruitt,K.D. and Tatusova,T. (2007) Entrez Gene: gene-centered information at NCBI. *Nucleic Acids Res.*, **35**, D26–D31.
6. Maglott,D., Ostell,J., Pruitt,K.D. and Tatusova,T. (2005) Entrez Gene: gene-centered information at NCBI. *Nucleic Acids Res.*, **33**, D54–D58.
7. Hubbard,T.J., Aken,B.L., Ayling,S., Ballester,B., Beal,K., Bragin,E., Brent,S., Chen,Y., Clapham,P., Clarke,L. *et al.* (2009) Ensembl 2009. *Nucleic Acids Res.*, **37**, D690–D697.
8. Amberger,J., Bocchini,C.A., Scott,A.F. and Hamosh,A. (2009) McKusick's online mendelian inheritance in man (OMIM). *Nucleic Acids Res.*, **37**, D793–D796.
9. Hamosh,A., Scott,A.F., Amberger,J., Bocchini,C., Valle,D. and McKusick,V.A. (2002) Online mendelian inheritance in man (OMIM), a knowledgebase of human genes and genetic disorders. *Nucleic Acids Res.*, **30**, 52–55.
10. Bajdik,C.D., Kuo,B., Rusaw,S., Jones,S. and Brooks-Wilson,A. (2005) CGMIM: automated text-mining of Online Mendelian Inheritance in Man (OMIM) to identify genetically-associated cancers and candidate genes. *BMC Bioinformatics*, **6**, 78.
11. Masseroli,M., Galati,O., Manzotti,M., Gibert,K. and Pinciroli,F. (2005) Inherited disorder phenotypes: controlled annotation and statistical analysis for knowledge mining from gene lists. *BMC Bioinformatics*, **6(Suppl. 4)**, S18.
12. Hishiki,T., Ogasawara,O., Tsuruoka,Y. and Okubo,K. (2004) Indexing anatomical concepts to OMIM Clinical Synopsis using the UMLS Metathesaurus. *In Silico Biol.*, **4**, 31–54.
13. Cantor,M.N. and Lussier,Y.A. (2004) Mining OMIM for insight into complex diseases. *Medinfo*, **11**, 753–757.
14. Freudenberg,J. and Propping,P. (2002) A similarity-based method for genome-wide prediction of disease-relevant human genes. *Bioinformatics*, **18(Suppl. 2)**, S110–S115.
15. van Driel,M.A., Bruggeman,J., Vriend,G., Brunner,H.G. and Leunissen,J.A. (2006) A text-mining analysis of the human phenome. *Eur. J. Hum. Genet.*, **14**, 535–542.
16. Nelson,S.J., Schopen,M., Savage,A.G., Schulman,J.L. and Arluk,N. (2004) The MeSH translation maintenance system: structure, interface design, and implementation. *Stud. Health Technol. Inform.*, **107**, 67–69.
17. Nakazato,T., Takinaka,T., Mizuguchi,H., Matsuda,H., Bono,H. and Asogawa,M. (2008) BioCompass: a novel functional inference tool that utilizes MeSH hierarchy to analyze groups of genes. *In Silico Biol.*, **8**, 53–61.
18. Jensen,L.J., Saric,J. and Bork,P. (2006) Literature mining for the biologist: from information retrieval to biological discovery. *Nat. Rev. Genet.*, **7**, 119–129.
19. Gaudan,S., Kirsch,H. and Rebholz-Schuhmann,D. (2005) Resolving abbreviations to their senses in Medline. *Bioinformatics*, **21**, 3658–3664.
20. Horsthemke,B. and Wagstaff,J. (2008) Mechanisms of imprinting of the Prader-Willi/Angelman region. *Am. J. Med. Genet. A*, **146A**, 2041–2052.
21. Rother,K.I. (2007) Diabetes treatment—bridging the divide. *N. Engl. J. Med.*, **356**, 1499–1501.
22. McKusick,V.A. (2007) Mendelian Inheritance in Man and its online version, OMIM. *Am. J. Hum. Genet.*, **80**, 588–604.

Carcinogenesis and cellular immortalization without persistent inactivation of p16/Rb pathway in lung cancer

MARINA ARIFIN[1], KEIJI TANIMOTO[1], ANDIKA CHANDRA PUTRA[1], EISO HIYAMA[2], MASAHIKO NISHIYAMA[1,3] and KEIKO HIYAMA[1]

[1]Department of Translational Cancer Research, Hiroshima University, Research Institute for Radiation Biology and Medicine (RIRBM); [2]Natural Science Center for Basic Research and Development, Hiroshima University, Hiroshima; [3]Translational Research Center, Saitama Medical University International Medical Center, Saitama, Japan

Received November 27, 2009; Accepted December 29, 2009

DOI: 10.3892/ijo_00000605

Abstract. Existence of cancer stem cells (CSCs) is still hypothetical and their practical marker is not available yet in lung cancer. To verify the possible existence of CSCs and to find their markers in lung cancer, we compared the p16/Rb and telomerase status in 83 lung cancer tissues and 15 lung cancer cell lines, since inactivation of p16/Rb pathway is considered to be a prerequisite for normal somatic cells to become immortal cancer cells. We found that 7 of 14 adenocarcinoma, but not squamous cell carcinoma, tissues with high telomerase activity and 3 adenocarcinoma cell lines likely had intact p16/Rb. Such cell lines showed higher colony formation capacity in soft agar compared with inactivated ones with similar growth rate. Moreover, cisplatin-resistant cell line PC9/CDDP with intact p16/Rb, but not PC14/CDDP with its inactivation, increased the colony formation capacity compared with the parent cells. Since CSCs are considered to be resistant to conventional anticancer drugs, they could have been concentrated as long as CSCs existed. We propose that half of immortal lung adenocarcinomas are derived from innately telomerase-positive stem cells, which might be the origin of CSCs, and that high telomerase activity with intact p16/Rb could be a marker of stem cell origin.

Introduction

The new concept describes a cancer stem cell (CSC) as a cell within a tumor that is able to self-renew and to produce the heterogenous lineages of cancer cells that comprise the tumor (1). Cancer stem cells have been speculated to be the source of many solid tumors including lung cancer (2), and be resistant to conventional chemo- and radio-therapy. Thus, identification of CSCs and their biomarkers in lung cancer is urgent to improve patient prognosis. Previously, CD133 (*PROM1*: prominin-1) positive cells (2,3), side population cells that extrude Hoechst 33342 dye (4), or aldehyde dehydrogenase positive cells (5) have been demonstrated to be the fractions of putative CSCs in malignant tumors including lung cancer, but they are still not conclusive (6).

It is widely accepted that CSCs have telomerase activity and are immortal so that they can produce cancer cells indefinitely (7-9). But it is not clear yet whether CSCs originate from normal stem cells or from differentiated somatic cells. Since human somatic cells are required to inactivate p16/Rb pathway to overcome cellular senescence and become immortal cancer cells concomitant with activation of telomerase (10,11), we hypothesized that immortal cancer cells without inactivation of p16/Rb pathway could not be derived from usual somatic cells, but be originated from innately telomerase-positive cells, i.e., stem cells. We previously found that all examined squamous cell carcinoma and small cell lung cancer (SCLC) tissues with high telomerase activity, meaning immortal cancer cells, had aberrations in *RB1* and/or *TP53* genes. However, in lung adenocarcinomas with high telomerase activity, neither gene was found in half of the samples (12). To verify this hypothesis, we examined p16 status in 83 lung cancer tissues and 15 lung cancer cell lines, and compared the relationship between the p16/Rb pathway status and the telomerase activity levels or colony formation capacities.

Materials and methods

Tumor samples. A total of 83 surgically resected primary lung cancer tissues, including 42 adenocarcinomas, 30 squamous cell carcinomas, 4 adenosquamous cell carcinomas, and 7 SCLCs, were obtained from chemotherapy-naïve patients, as well as the corresponding adjacent non-cancer lung tissue samples as controls. All tissues had been provided by the Department of Pathology and Department of Molecular and Internal Medicine, Hiroshima University between 1991-1996. Their pathological stages had been assessed according to the International Staging System (13) and telomerase activity, *RB1* loss of heterozygosity (LOH), *TP53* LOH, and chromo-

Correspondence to: Dr Keiko Hiyama, Department of Translational Cancer Research, Research Institute for Radiation Biology and Medicine, Hiroshima University, 1-2-3 Kasumi, Minami-ku, Hiroshima 734-8551, Japan
E-mail: khiyama@hiroshima-u.ac.jp

Key words: p16/Rb pathway, telomerase, cellular immortalization, cancer stem cells, lung cancer, adenocarcinoma

some 1p deletion mapping were previously reported (12,14-16). Written informed consent was obtained from all patients before surgery, and this study was approved by our Institutional Ethics Committee.

Cell lines. The SCLC cell line PC-6 and its SN-38- and CPT-11-resistant variants (SN2-5 and DQ2-2), a lung squamous cell carcinoma cell line LC-S, and lung adenocarcinoma cell lines PC-9 and PC-14 and their CDDP-resistant variants (PC-9/CDDP and PC-14/CDDP, respectively) as well as A549 were prepared and examined for CDDP sensitivity as previously described (17). The remaining 6 lung adenocarcinoma cell lines, RERF-LC-MS, VMRC-LCD, PC-3, RERF-LC-Ad1, RERF-LC-Ad2, and RERF-LC-KJ, and control fibroblast strain TIG-1 were obtained from the Health Science Research Resources Bank (Osaka, Japan).

Colony formation assay with soft agar. Anchorage-dependency of 11 lung adenocarcinoma cell lines was evaluated by conventional colony formation assay with soft agar in triplicate, as previous reported (18). Briefly, $5x10^3$ cells were cultured in 0.4% SeaPlaque GTG agarose (Bioproducts), and after 14 and 21 days of culture at 37°C with 5% CO_2, colony number was counted under microscopy for slow-growing cells (colonies containing >5 cells were counted) and macroscopically with crystal violet staining for rapid growing cells (colonies macroscopically visible were counted).

Preparation of DNA and RNA. For tissue samples, genomic DNA had been prepared previously (15). For cell lines genomic DNA and total RNA were extracted from the frozen cell pellets using QIAamp™ DNA Mini kit (Qiagen Inc., Valencia, CA) and Qiagen RNeasy™ mini kit (Qiagen), respectively, according to the manufacturer's protocols.

Real-time RT-PCR for evaluation of mRNA levels. For cell lines, 2 μg of total RNA was reverse-transcribed using High-Capacity cDNA Archive™ Kit (Applied Biosystems, Foster City, CA, USA). An aliquot of the cDNA (equivalent to 10 ng total RNA) was subjected to each real-time RT-PCR using Universal Probe Library (UPL, Roche Diagnostics, Tokyo, Japan) for *CDKN2A* (p16), *PROM1*, *BMI1*, and *ABCG2*, TaqMan Gene Expression Assays for *RB1* (Hs00153108_m1 targeting exons 24-25, Applied Biosystems), and Pre-Developed TaqMan Assay Reagents (Applied Biosystems) for ACTB as an internal control. Each reaction was carried out in duplicate or triplicate using ABI PRISM™ 7900HT Sequence Detection System (Applied Biosystems) and relative gene expression levels calculated as ratio to *ACTB* expression level were standardized using a pooled cDNA derived from 17 various cancer cell lines. The UPL primers (final concentration 200 nM each) and MGB-probe (final concentration 100 nM) sets are as follows: *CDKN2A*-F: 5'-GTGGACCTGGCTGAG GAG-3'. *CDKN2A*-R: 5'-CTTTCAATCGGGGATGTCTG-3'. *CDKN2A*-probe: UPL no. 34 (Roche). *PROM1*-F: 5'-AACCT TACACGAGCAAGGAATTA-3'. *PROM1*-R: 5'-AAACTTG TTCAAAAGTGAGCTTCAT-3'. *PROM1*-probe: UPL no. 48 (Roche). *BMI1*-F: 5'-TTCTTTGACCAGAACAGATTGG-3'. *BMI1*-R: 5'-GCATCACAGTCATTGCTGCT-3'. *BMI1*-probe: UPL no. 63 (Roche). *ABCG2*-F: 5'- TGGCTTAGACTCAAG CACAGC-3'. *ABCG2*-R: 5'-TCGTCCCTGCTTAGACA TCC-3'. *ABCG2*-probe: UPL no. 56 (Roche).

Real-time PCR for quantitation of DNA amounts. Homozygous deletion of *CDKN2A* was determined by TaqMan™ quantitative real-time PCR system with TagMan Universal PCR master mix and the ABI PRISM™ 7900HT Sequence Detection System (Applied Biosystems) using *TFRC* as control gene amount (12). Using a 384-well reaction plate (Applied Biosystems), 20 ng of genomic DNA and 2 sets of primers (final concentration 200 nM each for *CDKN2A* and 300 and 900 nM for *TFRC* forward and reverse primers, respectively) and fluorescent-probes (final concentration 100 nM for FAM-labeled *CDKN2A* and 200 nM for VIC-labeled *TFRC*) were mixed in a 10-μl reaction mixture. The primer and probe set for *TFRC* was previously reported (12) and that for *CDKN2A* is as follows: *CDKN2A*-F: 5'-AGCTTCCTTTCCGTCA TGC-3'. *CDKN2A*-R: 5'-TCATGACCTGCCAGAGAGAA-3'. *CDKN2A*-probe: UPL no. 21 (Roche). Threshold cycle (Ct) for each gene was determined using thermocycler software and the average of 3 independent Cts was calculated. Standard DNA was prepared by mixing genomic DNAs derived from two samples, non-cancer cells with intact *CDKN2A* and a cancer cell line with homologous deletion, at 10:0 (STD-100%), 8:2 (-80%), 6:4 (-60%), 4:6 (-40%), 2:8 (-20%), and 0:10 (0%).

Fragment analysis for detection of LOH. LOH of *CDKN2A* was evaluated by fragment length analysis using microsatellite marker D9S1748. The FAM-labeled forward primer (5'-CACCTCAGAAGTCAGTGAGT-3') and a non-labeled reverse primer (5'-GTGCTTGAAATACACCTTTCC-3') were mixed with 20 ng of genomic DNA and subjected to PCR followed by fragment analysis using ABI PRISM 310 Genetic Analyzer and GeneScan™ software as previously described (12). The adjacent non-cancer lung tissue samples were used as controls of peak height ratio of the corresponding repeat numbers.

Fragment analysis for quantitative methylation-specific PCR (qMSP). MSP was carried out to evaluate the *CDKN2A* (p16) CpG island methylation status according to a previous report (19) with quantitative modification. The bisulfite-treated genomic DNA was first amplified with outside non-fluorescent primers (35 cycles, annealing at 60°C) and then nested PCR was carried out using FAM-labeled methylated or HEX-labeled unmethylated allele-specific primers with annealing temperature at 65°C. Then, 0.5 μl each of methylated (FAM labeled) and unmethylated (HEX labeled) PCR products were mixed and subjected to ABI PRISM 310 Genetic Analyzer (Applied Biosystems). The methylation ratio was calculated as (area of FAM peak)/(areas of FAM peak + HEX peak).

Direct sequence analysis for RB1 cDNA. cDNAs derived from the 15 lung cancer cell lines were subjected to PCR using 2 sets of primers amplifying exons 10-26 that cover almost all naturally occurring *RB1* mutations. The PCR condition was 95°C for 15 min followed by 40 cycles of 95°C for 30 sec, 58°C for 1 min, and 72°C for 90 sec. Sequence analyses were carried out using Big Dye Terminator v1.1 Cycle Sequencing

Table I. The genetic aberrations in 83 primary lung cancers.

No.	Gender	Age	Stage	Tel[a]	*TP53*[a]	*RB1*[a]	1p34[a]	*CDKN2A* HD/LOH	*CDKN2A* qMSP	p16/Rb inactivation
Adenocarcinoma										
1	F	61	I	Low	Hetero	Hetero	Hetero	Hetero	1.0	+
2	M	69	I	Low	Hetero	Hetero	Hetero	Hetero	1.0	+
3	M	75	I	Low	Hetero	Hetero	Hetero	Hetero	1.0	+
4	M	62	I	Low	Hetero	Hetero	Hetero	Hetero	1.0	+
5	M	66	I	Low	Hetero	Hetero	Hetero	Hetero	1.0	+
6	F	67	I	Low	Hetero	Hetero	Hetero	Hetero	0.80	+
7	F	67	II	Low	Hetero	Hetero	Hetero	Hetero	1.0	+
8	M	76	IIIA	Low	Hetero	Hetero	Hetero	Hetero	0.99	+
9	M	61	IIIA	Low	Hetero	Hetero	Hetero	NI	1.0	+
10	M	60	IIIB	Low	Hetero	Hetero	Hetero	Hetero	0.27	+
11	F	64	IV	Low	Hetero	Hetero	Hetero	HD	0	+
12	F	56	IV	Low	Hetero	Hetero	Hetero	NI	0.59	+
13	F	57	IIIA	Low	Hetero	Hetero	LOH	NI	1.0	+
14	M	60	IV	Low	Hetero	Hetero	LOH	Hetero	1.0	+
15	F	65	IV	Low	Hetero	Hetero	LOH	LOH	0.88	+
16	F	62	I	Low	Hetero	LOH	LOH	Hetero	0.28	+
17	F	60	I	Low	NI	Hetero	Hetero	Hetero	0.90	+
18	M	48	I	Low	NI	Hetero	LOH	NI	1.0	+
19	F	51	IIIa	Low	NI	Hetero	Hetero	Hetero	1.0	+
20	F	57	I	Low	LOH	Hetero	LOH	LOH	0.69	+
21	M	58	IV	Low	LOH	Hetero	Hetero	Hetero	1.0	+
22	F	56	IV	Low	LOH	Hetero	Hetero	Hetero	1.0	+
23	M	66	IV	Low	LOH	Hetero	Hetero	Hetero	1.0	+
24	F	72	IIIA	Low	LOH	LOH	Hetero	Hetero	0.97	+
25	M	67	I	Low	LOH	LOH	LOH	Hetero	0.94	+
26	M	77	I	Low	LOH	LOH	LOH	NI	0.11	+
27	M	64	I	Low	LOH	LOH	LOH	Hetero	0.84	+
28	M	62	IIIA	Low	LOH	LOH	LOH	NI	0.10	+
29	F	78	I	High	Hetero	Hetero	Hetero	Hetero	0	-
30	M	69	I	High	Hetero	Hetero	Hetero	Hetero	0.87	+
31	M	62	I	High	Hetero	Hetero	Hetero	Hetero	0.11	-
32	M	75	I	High	Hetero	Hetero	Hetero	NI	0	-
33	F	62	II	High	Hetero	Hetero	Hetero	Hetero	0	-
34	F	69	IIIA	High	Hetero	Hetero	Hetero	Hetero	0.07	-
35	F	77	IV	High	Hetero	Hetero	Hetero	HD	0	+
36	F	80	I	High	Hetero	LOH	Hetero	Hetero	0	+
37	F	59	IIIA	High	LOH	Hetero	Hetero	Hetero	0.13	-
38	M	76	IIIA	High	LOH	Hetero	LOH	Hetero	0.15	-
39	M	55	I	High	LOH	LOH	LOH	HD	0	+
40	M	68	II	High	LOH	LOH	LOH	Hetero	0.10	+
41	M	66	IV	High	LOH	LOH	Hetero	Hetero	0.12	+
42	M	50	IIIB	High	LOH	LOH	LOH	Hetero	0	+
Adenosquamous cell carcinoma										
43	M	75	IIIA	Low	Hetero	Hetero	Hetero	HD	0	+
44	M	42	I	Low	NI	LOH	Hetero	NI	1.0	+
45	M	75	IV	Low	LOH	LOH	Amp	LOH	1.0	+
46	M	69	IIIA	High	LOH	LOH	LOH	HD	0.21	+

Table I. Continued.

No.	Gender	Age	Stage	Tel[a]	*TP53*[a]	*RB1*[a]	1p34[a]	*CDKN2A* HD/LOH	*CDKN2A* qMSP	p16/Rb inactivation
Small cell lung cancer										
47	M	75	I	Low	LOH	Hetero	LOH	Hetero	0	-
48	F	79	II	High	LOH	Hetero	Hetero	Hetero	0	-
49	M	56	I	High	LOH	LOH	Amp	Hetero	0	+
50	M	71	IIIA	High	LOH	LOH	Amp	Hetero	0.28	+
51	M	77	IIIA	High	LOH	LOH	Hetero	Hetero	0	+
52	M	74	I	High	LOH	LOH	LOH	HD	0	+
53	M	74	II	High	LOH	LOH	LOH	Hetero	0	+
Squamous cell carcinoma										
54	M	74	I	Low	Hetero	Hetero	Hetero	NI	0	-
55	F	62	I	Low	Hetero	Hetero	LOH	Hetero	0	-
56	M	70	II	Low	Hetero	Hetero	Hetero	NI	0	-
57	M	69	II	Low	Hetero	Hetero	Hetero	NI	0	-
58	M	63	II	Low	Hetero	Hetero	Hetero	Hetero	0	-
59	M	52	IIIA	Low	Hetero	Hetero	Hetero	Hetero	0	-
60	M	79	IIIA	Low	Hetero	Hetero	Hetero	Hetero	0	-
61	M	70	IIIA	Low	Hetero	Hetero	Hetero	LOH	0	+
62	M	69	IIIA	Low	Hetero	LOH	Hetero	LOH	0	+
63	M	77	IIIB	Low	Hetero	LOH	LOH	Hetero	0	+
64	M	61	II	Low	NI	Hetero	LOH	Hetero	0	-
65	M	72	I	Low	LOH	Hetero	Hetero	Hetero	NI	-
66	M	67	I	Low	LOH	Hetero	Hetero	LOH	0	+
67	M	60	IV	Low	LOH	Hetero	LOH	NI	0	-
68	M	71	I	Low	LOH	Hetero	LOH	HD	0	+
69	M	73	I	Low	LOH	LOH	Hetero	HD	0	+
70	M	87	I	Low	LOH	LOH	Hetero	Hetero	0	+
71	M	65	IIIA	Low	LOH	LOH	Hetero	LOH	0	+
72	F	71	I	Low	LOH	LOH	LOH	Hetero	0	+
73	M	63	I	Low	LOH	LOH	LOH	LOH	0	+
74	M	64	IIIA	Low	LOH	LOH	LOH	HD	NI	+
75	M	73	IV	Low	LOH	NI	Hetero	Hetero	0	-
76	M	66	I	Low	LOH	NI	LOH	Hetero	0	-
77	M	65	IIIA	Low	LOH	NI	LOH	LOH	0.02	-
78	M	72	IIIB	High	Hetero	LOH	LOH	LOH	0	+
79	M	62	IIIB	High	Hetero	LOH	LOH	Hetero	0	+
80	M	67	IIIA	High	LOH	Hetero	LOH	HD	0	+
81	M	62	IIIA	High	LOH	LOH	Hetero	HD	0	+
82	M	53	IV	High	LOH	LOH	LOH	NI	0	+
83	M	71	I	High	LOH	NI	LOH	HD	NI	+

[a]Previously analyzed for Tel (telomerase activity level), *TP53* (LOH in *TP53*), *RB1* (LOH in *RB1*), 1p34 (deletion within 1p34 to pter) (12,14-16). qMSP, (methylated allele peak)/(methylated + unmethylated allele peaks) area ratio >0.25 was considered as methylated; HD, homologous deletion; NI, not informative.

Kit™ and ABI PRISM 310 or PRISM 3100 Genetic Analyzer (Applied Biosystems). The 2 set primers are: *RB1*set1ex9-F: 5'-CTAATGGACTTCCAGAGGTTG-3'. *RB1*set1ex20-R: 5'-CGGAGATAGGCTAGCCGATA-3'. *RB1*set2ex19-F:

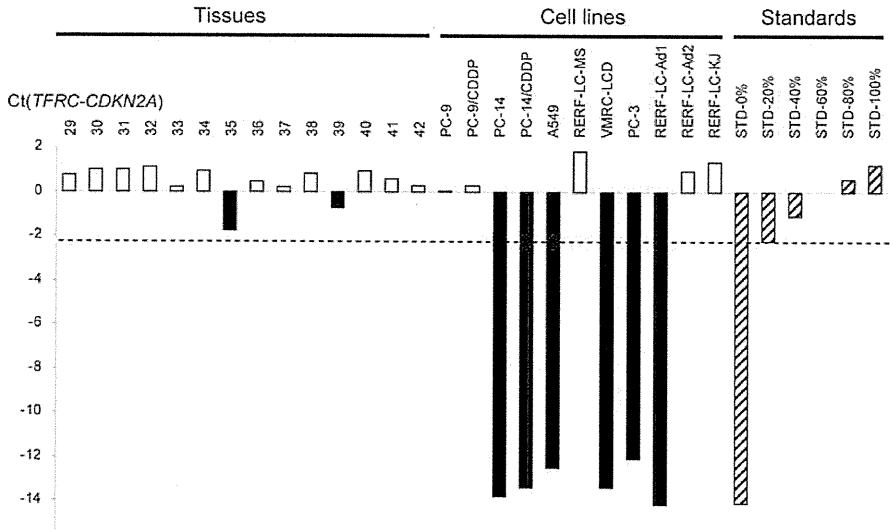

Figure 1. Detection of homologous deletion of p16 by quantitative real-time PCR for *CDKN2A* using control gene *TFRC* in representative samples (all adenocarcinoma tissues with high telomerase activity and lung adenocarcinoma cell lines). Tissue samples were classified as having homologous deletion when Ct(*TFRC*)-Ct(*CDKN2A*) in each sample < STD-60% (= 0, smooth line), and cell lines when < STD-20% (= -2.25, dotted line). Ct, threshold cycles; Hatched bar, standard DNA for quantitation; Closed bar, classified as homologous deletion; Open bar, classified as retaining at least one allele.

5'-TACTGCAAATGCAGAGACAC-3'. *RB1*set2ex27-R: 5'-GAAGAGGAAACAATCTGCTA-3'.

Telomerase activity and other genetic aberrations. Among the genetic aberrations in the tissue samples summarized in Table I, we previously evaluated and reported the telomerase activity level by TRAP assay (14), 1p34 LOH by deletion mapping using 12 polymorphic markers (16), and LOH of *TP53* and *RB1* genes using 5 and 4 polymorphic markers, respectively (12,15).

Statistical analysis. All statistical tests were performed using StatView version 5.0 software (SAS Institute Inc., Cary, NC, USA), and the Student's t-test, χ^2, or Fisher's exact test was used to determined the P-value. Differences of $P<0.05$ were considered statistically significant.

Results

Telomerase activity levels and LOH of *TP53*, *RB1*, and 1p34 locus in the lung cancer tissues have been evaluated previously (12,14-16) and summarized in Table I with the present data.

p16 inactivation. Persistent type inactivation of p16 was evaluated by the existence of *CDKN2A* homozygous deletion, LOH, and/or promoter methylation in 83 lung cancer tissues, and by *CDKN2A* homozygous deletion or complete promoter methylation in 15 lung cancer cell lines.

Homozygous deletion, [threshold cycles (Ct) of *TFRC*]-(Ct of *CDKN2A*) was smaller in a sample than that of 60% (for tissue samples) or 20% (for cell lines) standards in real-time PCR considering the existence of contaminated non-cancer cells in tissue samples, was found in 3 adenocarcinoma, 6 squamous cell carcinoma, 2 adenosquamous cell carcinoma, and 1 SCLC tissues and 6 adenocarcinoma cell lines (Fig. 1) and 1 squamous cell carcinoma cell line, LC-S. LOH, i.e., the calculated peak height ratio of the 2 alleles was <70% or >150% of that in normal counterpart in fragment analysis, was found in 10 tissue samples (Fig. 2). Cell lines could not be analyzed for LOH due to the lack of normal counterpart.

For evaluating *CDKN2A* promoter methylation, we considered it methylated when the methylated allele ratio, (methylated allele peak area)/(methylated and unmethylated allele peak areas), was >25%, and complete methylation when the ratio was >80% (Fig. 3). The *CDKN2A* promoter methylation was detected in 61.9% (26/42) of adenocarcinoma, but none of squamous cell carcinomas. For lung cancer cell lines, RERF-LC-MS was completely methylated among the 8 cell lines that retained *CDKN2A* gene. Thus, p16 inactivation by deletion or promoter methylation is summarized in Tables II and III, and such inactivation in adenocarcinoma tissues revealed to be highly associated with low/nil telomerase activity (P=0.0001).

Rb inactivation. Inactivation of Rb was evaluated by the existence of *RB1* LOH (analyzed for 1 RFLP and 3 microsatellite loci) in 83 lung cancer tissues and by the existence of genetic aberrations in *RB1* cDNA (sequence analysis of exons 10-27, that cover the mutation hot-spot region) or absence of *RB1* mRNA detection (real-time RT-PCR) in the 15 lung cancer cell lines.

For the 83 lung cancer tissue samples, we previously analyzed and reported that *RB1* LOH was found in 26 (34.2%) of 76 non-small cell lung cancer (NSCLC) and 5 (71.4%) of 7 SCLC tissues (12,15). Among the 15 lung cancer cell lines examined, *RB1* expression could not be detected in 1 adenocarcinoma cell line, RERF-LC-KJ (Fig. 4A). Also by sequence analysis of *RB1* cDNA, only this cell line was revealed to have an aberration, an inframe deletion of 174 nucleotides by splicing out the entire exons 24 and 25.

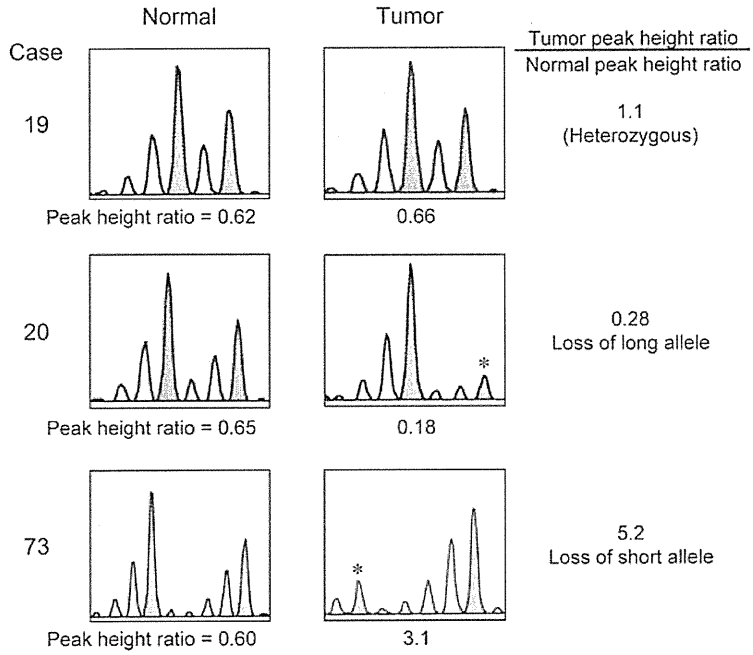

Figure 2. Detection of LOH of p16 by fragment analysis in representative samples. LOH, in cancer tissues was defined when the peak height ratio of heterozygous bands was <0.7 or >1.5 of expected ratio calculated from the normal counterpart. *Deleted allele demonstrating low peak possibly derived from contaminated non-cancer cells.

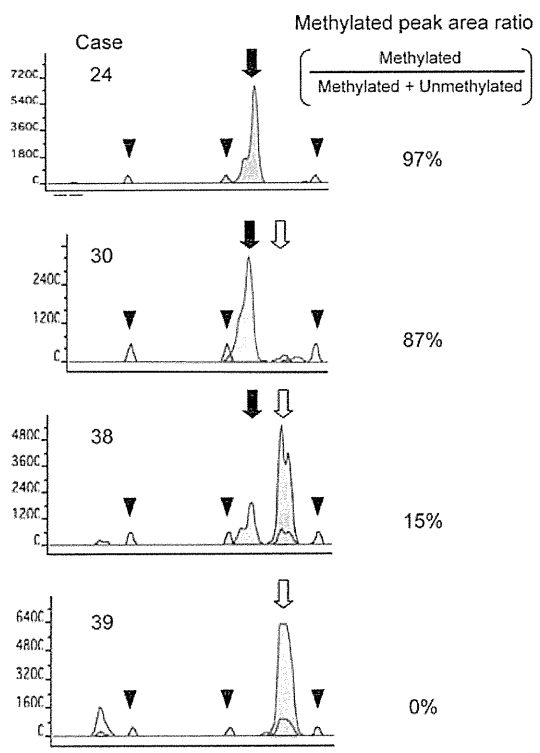

Figure 3. Quantitative evaluation of promoter methylation of p16 by fragment analysis in representative adenocarcinoma tissues. Methylated allele was labeled with FAM (closed arrow) and unmethylated allele was labeled with HEX (open arrow). The methylation ratio was calculated as (area of FAM peak)/(sum of areas of FAM & HEX peaks), and >25% was considered to be methylated and >80% as completely methylated. Arrowhead, size marker.

Inactivation of p16/Rb pathway. Combining above, inactivation of p16/Rb pathway, i.e., deletion/methylation of p16 and/or LOH of *RB1*, among the 83 lung cancer tissues was found in all 28 (100%) with low/nil telomerase activity but in only 7 of 14 (50%) with high telomerase activity (P=0.0001) in adenocarcinomas, whereas this relationship was the opposite in the remaining histology tumors (P=0.0309) (Table II). The p16 inactivation was inversely correlated with *RB1* LOH in adenocarcinoma tissues (P=0.0488).

Among the 15 lung cancer cell lines, the Rb inactivated cell line RERF-LC-KJ showed intact p16 as expected. Among the 11 adenocarcinoma cell lines, the p16/Rb pathway was considered to be intact in PC-9, its CDDP resistant variant PC-9/CDDP, and RERF-LC-Ad2 (p16/Rb pathway intact group) and inactivated in the remaining 8 cell lines (inactivated group). Then, cellular growth rate and colony formation capacity were carried out between these 2 groups.

Expression of cancer stem cell markers. As known cancer stem cell markers, we evaluated mRNA expression levels of *PROM1* (CD133), *BMI1*, and *ABCG2* by real-time RT-PCR in the 15 lung cancer cell lines. While the expression levels of *BMI1* and *ABCG2* genes were comparable among the all cell lines except for *ABCG2* in the drug resistant SCLC clones, *PROM1* was highly expressed in RERF-LC-Ad2, in which the p16/Rb pathway was considered to be intact (Fig. 4B).

Growth rate of adenocarcinoma cell lines. We found that the 11 adenocarcinoma cell lines can be divided into 2 groups according to their growth rates: >20 times multiplied at day 5 (rapid growth group, Fig. 5A) and less than that (slow growth group, Fig. 5B). The p16/Rb-intact cell lines PC-9 and PC-9/

Table II. Inactivation of p16/Rb in 83 lung cancer tissues.

Histology	Telomerase activity[a]	*RB1* LOH[a]	p16 inactivation	p16 and/or Rb inactivation
Adenocarcinoma				
	High (n=14)	5 (35.7%)	3 (21.4%)	7 (50%)
	Low/nil (n=28)	6 (21.4%)	26 (92.9%)	28 (100%)
Adenosquamous cell carcinoma				
	High (n=1)	1 (100%)	1 (100%)	1 (100%)
	Low/nil (n=3)	2 (66.7%)	3 (100%)	3 (100%)
Squamous cell carcinoma				
	High (n=6)	4 (66.7%)	4 (66.7%)	6 (100%)
	Low/nil (n=24)	8 (33.3%)	9 (37.5%)	12 (50.0%)
Small cell lung cancer				
	High (n=6)	5 (83.3%)	2 (33.3%)	5 (83.3%)
	Low/nil (n=1)	0 (0%)	0 (0%)	0 (0%)

[a]Previously analyzed for telomerase activity level and *RB1* LOH (12,14-16).

Table III. Inactivation of p16/Rb in lung cancer cell lines.

	Rb inactivation		p16 inactivation		
Histology	RT-PCR[a]	Deletion	HD	qMSP	p16/Rb inactivation
Adenocarcinoma					
PC-9	-	-	-	0.46	-
PC-9/CDDP	-	-	-	0.40	-
PC-14	-	-	+	NI	+
PC-14/CDDP	-	-	+	NI	+
A549	-	-	+	NI	+
RERF-LC-MS	-	-	-	1.0	+
VMRC-LCD	-	-	+	NI	+
PC-3	-	-	+	NI	+
RERF-LC-Ad1	-	-	+	NI	+
RERF-LC-Ad2	-	-	-	0	-
RERF-LC-KJ	+	+	-	0	+
Squamous cell carcinoma					
LC-S	-	-	+	NI	+
Small cell lung cancer					
PC-6	-	-	-	0.01	-
SN2-5	-	-	-	0.04	-
DQ2-2	-	-	-	0.16	-

[a]RT-PCR +, not detectable by real-time RT-PCR; qMSP, methylation ratio >0.8 was considered as completely inactivated; HD, homologous deletion; NI, not informative.

CDDP in the former group and RERF-LC-Ad2 in the latter group did not show accelerated growth compared to the inactivated ones in each group.

Colony formation assay with soft agar. While the colonies in the rapid growth group were evaluated macroscopically after crystal violet staining (Figs. 5C and 6), those in the slow

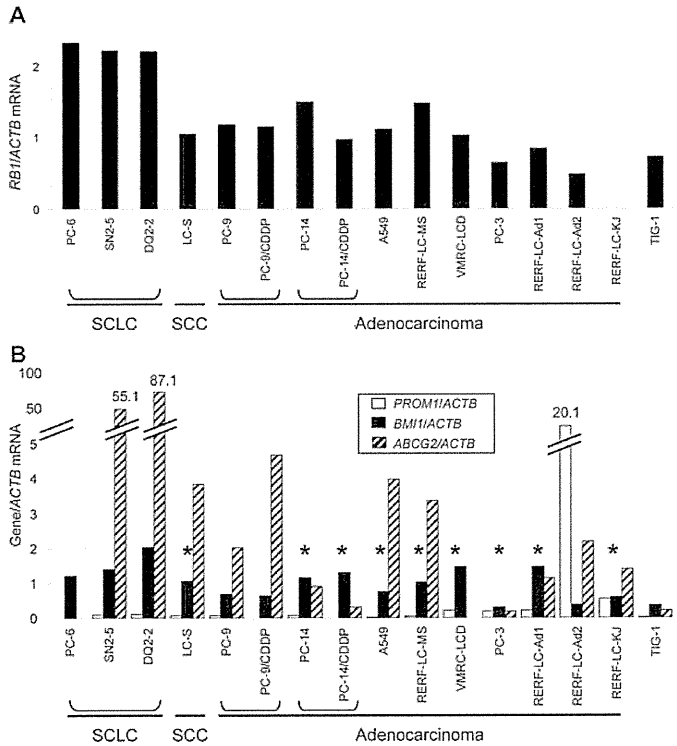

Figure 4. mRNA expression levels in all 15 cell lines evaluated by real-time RT-PCR using *ACTB* as internal control. *RB1* was not detected in RERF-LC-KJ (A). *PROM1* (open bar) was highly expressed in RERF-LC-Ad2, while the expression levels of *BMI1* (closed bar) and *ABCG2* (hatched bar) genes were comparable except for the drug resistant SCLC clones for *ABCG2* (B). Cell lines inactivated for p16/Rb pathway (homologous deletion or complete methylation of p16 or complete inactivation of *RB1*) are indicated by asterisk. TIG-1 is a non-cancer control human fibroblasts.

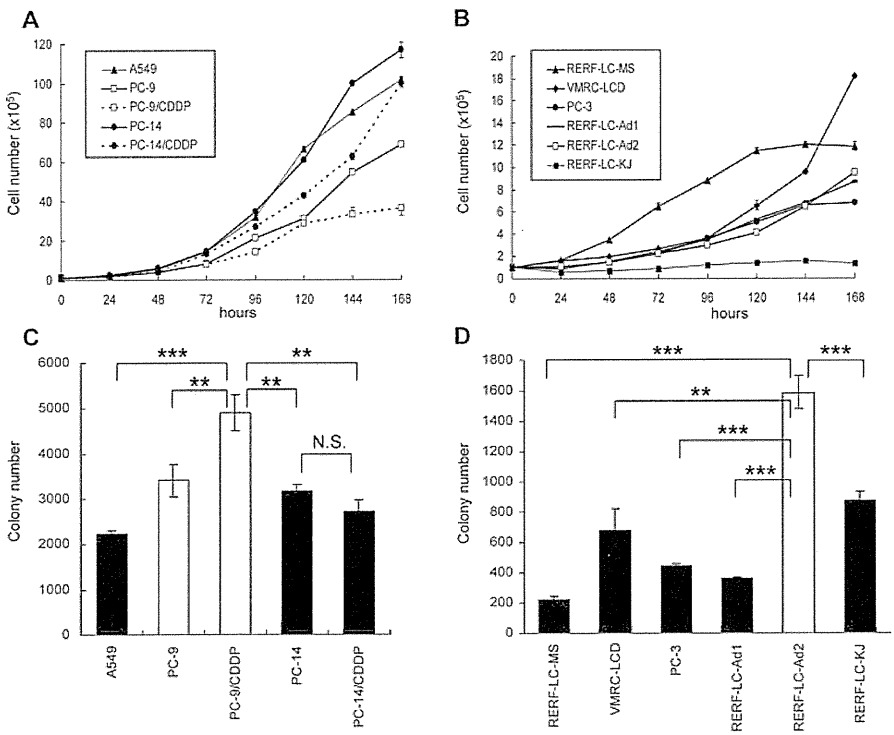

Figure 5. Growth rate and colony numbers in colony formation assay for the 11 lung adenocarcinoma cell lines. In each 60-mm diameter dish, 10^5 each of rapid growth cell lines (A) or slow growth cell lines (B) were cultured, and cell number was calculated every day for 1 week in triplicate. Colony numbers of the rapid growth cell lines were evaluated macroscopically after crystal violet staining (C) while those of the slow growth cell lines were evaluated microscopically (D). p16/Rb intact cell lines (open box) did not show higher growth but showed increased colonies (open bar) in soft agar compared to p16/Rb inactivated cell lines (closed bar) in each group. $^{**}P<0.01$; $^{***}P<0.001$; N.S., not significant.

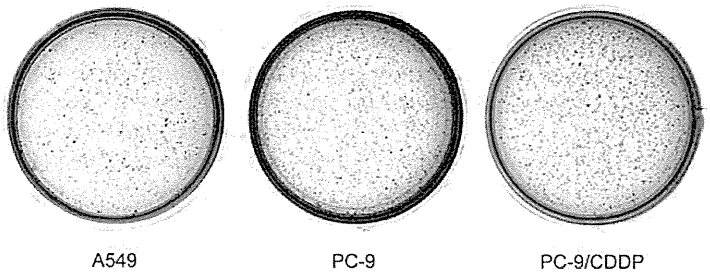

Figure 6. Colony formation assay for representative adenocarcinoma cell lines with rapid growth. Macroscopically visible colonies shown after crystal violet staining are p16/Rb inactivated cell line A549 < p16/Rb intact PC-9 < CDDP resistant PC-9 variant PC-9/CDDP.

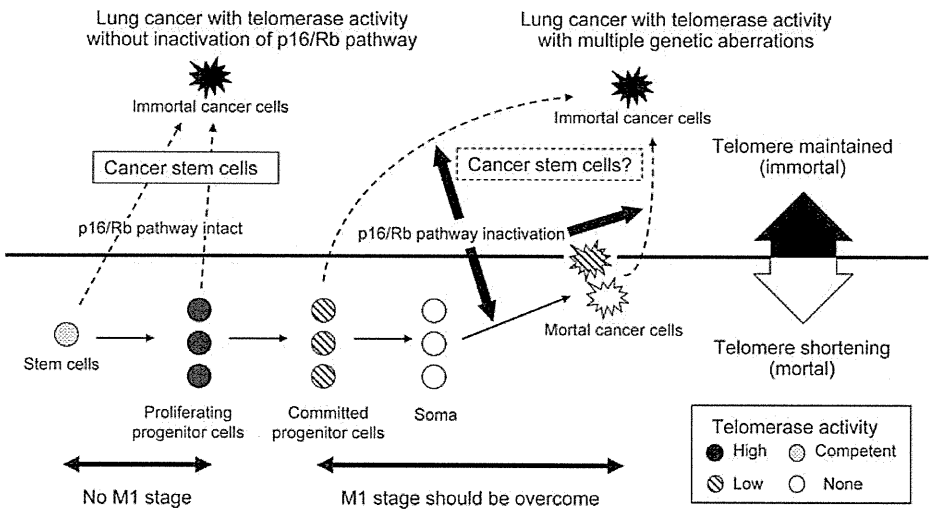

Figure 7. Our hypothesis of lung carcinogenesis. Immortal lung cancer cells might be derived from either of the two pathways: developed from telomerase positive normal cells, i.e., stem cells, through cancer stem cells or from telomerase negative somatic cells through multiple clonal selections acquiring genetic aberrations including *TP53*, *CDKN2A*, and *RB1* inactivations and telomerase activation, but not necessarily through cancer stem cells. Half of lung adenocarcinomas with high telomerase activity may develop from the former pathway, while most of squamous cell carcinomas develop from the latter pathway. M1, mortality stage 1; M2, mortality stage 2.

growth group were evaluated microscopically before staining, since they were small and macroscopically invisible in general even after 3 weeks (Fig. 5D). The p16/Rb intact cell lines, PC-9 and PC-9/CDDP in the rapid growth group and RERF-LC-Ad2 in the slow growth group, showed significantly higher colony formation capacity than the p16/Rb inactivated cell lines in each group ($P<0.01$-$P<0.0001$). Moreover, CDDP-resistant clone with intact p16/Rb (PC-9/CDDP), but not that with p16/Rb inactivation (PC-14/CDDP), showed significantly higher colony formation capacity than the parent clone ($P<0.001$, Figs. 5C and 6).

Discussion

Most malignant tumors must have a mechanism for bypassing senescence to acquire the unlimited proliferative capacity that is required for advanced cancers. Human somatic cells are considered to have two stages of checkpoint before acquiring immortality (two-stage model for cellular senescence): mortality stage 1 (M1) that can be overcome by inactivation of p16/Rb and p53 pathways and mortality stage 2 (M2), that requires activation of telomerase to be overcome (11,20). In fact, we previously found that all examined lung squamous cell carcinoma and SCLC tissues with high telomerase activity had aberrations in *RB1* and/or *TP53* genes. However, in lung adenocarcinomas with high telomerase activity, neither gene was found in half of them (12). We also showed that cancer tissues with high telomerase activity consisted of predominantly telomerase positive cells, i.e., immortal cancer cells, while those with low telomerase activity consisted of predominantly telomerase negative cells (21), and lung cancer cell lines always showed high telomerase activity (14). In addition, we confirmed full-length type *TERT* mRNA expression in all 15 lung cancer cell lines used in the present study by real-time RT-PCR, which had been confirmed to correlate with telomerase activity (22). Since we previously found that lung cancers which might have originated from telomerase positive bronchial epithelia always showed high telomerase activity (23), lung cancers with high telomerase activity, consist of predominantly immortal cancer cells, and immortal lung cancer cell lines might have been derived from either of the two pathways:

developed from telomerase positive normal cells, i.e., stem cells, or from telomerase negative somatic cells through multiple clonal selections acquiring genetic aberrations including *TP53*, *CDKN2A*, and/or *RB1* inactivation and telomerase activation.

To confirm this hypothesis, we examined incidence of persistent type p16 inactivation (deletion and/or methylation of *CDKN2A*) in the tissue samples as well as p16/Rb status and colony formation capacity in cell lines in the present study. It has been reported that the inactivation of p16 occurs most prominently through promoter methylation or homozygous deletion and less often through mutation in lung cancers (24). As we speculated, persistent inactivation of p16/Rb pathway, deletion of *CDKN2A* or *RB1* or methylation of *CDKN2A* promoter, was found in all adenocarcinoma tissues with low/nil telomerase activity, while neither was found in half of adenocarcinomas with high telomerase activity (P=0.0001). For other genetic aberrations, we previously reported that the *RB1* LOH was associated with *TP53* and 1p34 LOH but not with *EGFR* aberrations (12). In the present study, 5 of 7 p16/Rb intact adenocarcinomas with high telomerase activity also lacked the *TP53* LOH and 4 of them lacked both *TP53* and 1p34 LOH (Table I), indicating that these cases have escaped the M1 stage without persistent inactivation of p16/Rb pathway, p53 pathway, and the unknown pathway involving 1p34 locus. The importance of the p16/Rb and p53 pathways in lung epithelial cells is known by the high incidence of their defects in any histological type of lung cancer (25), and the adenocarcinomas without their persistent inactivation may have come without these checkpoints.

It has been indicated that only a small proportion of the tumor cells are able to form colonies in an *in vitro* colonogenic assay (26), and we found that adenocarcinoma cell lines without persistent inactivation of p16/Rb pathway had higher colony formation capacity in soft agar. Moreover, CDDP-resistant clone with intact p16/Rb (PC-9/CDDP), but not one with inactivation (PC-14/CDDP), showed higher colony formation capacity than the parent clones. Although the evidence is not sufficient yet, this could be explained that the former contained CSCs and enriched them in the CDDP-resistant clone, because CSCs are considered to be resistant to conventional chemotherapeutic drugs (2), while the latter did not contain CSCs originally and could not enrich the resistant clone. We also examined the expression levels of the known cancer stem cell markers, *PROM1* (2), *BMI1* (7), and *ABCG2* (27) in 15 lung cancer cell lines, and found that the p16/Rb intact cell line RERF-LC-Ad2 showed markedly high expression of *PROM1*, supporting our hypothesis that the p16/Rb intact immortal cancer cells may have derived from stem cells, and none of the presently available CSC markers is sufficient for all types of lung cancer.

Taken together, the present data indicate that 7 (50%) of 14 lung adenocarcinoma tissues with high telomerase activity (indicating they are predominantly consist of immortal cancer cells) and 3 of 11 (or 2 of 9 parent) lung adenocarcinoma cell lines, PC-9, PC-9/CDDP, and RERF-LC-Ad2, may have developed from M1 escaped cells, i.e., innately telomerase-positive stem cells, which are considered to be the origin of CSCs. Some of SCLC may have derived from such cells, because 1 of 6 SCLC tissues with high telomerase activity and 1 original (PC-6) as well as its 2 drug-resistant cell clones showed intact p16/Rb pathway (Fig. 7). However, for squamous cell carcinoma, no tissue with high telomerase activity nor the cell line examined showed intact p16/Rb pathway, indicating that it is always required to overcome the M1 stage to become immortal squamous cell carcinoma cells and that the telomerase-negative somatic cells may be of such origin. This speculation may be partly supported by the facts that squamous cell carcinoma often demonstrates evidence of multistep carcinogenesis, i.e., hyperplasia, metaplasia, dysplasia, carcinoma *in situ*, and invasive cancer, while adenocarcinoma and SCLC often lack such precancerous lesions indicating *de novo* carcinogenesis. Thus, we propose that there are two distinct pathways in lung carcinogenesis: one from primarily telomerase-positive cells, i.e., stem cells, independent of p16/Rb checkpoint mechanism in M1 stage, while the other from telomerase-negative somatic cells overcoming the M1 stage by inactivation of the p16/Rb and p53 pathways.

In conclusion, our study showed new important insights into lung CSCs. In particular, high telomerase expression without p16/Rb aberration possibly is a marker of cancer stem cells in lung cancers. Although further experiments are necessary to confirm our hypothesis, it could be an important key to study the molecular mechanisms of lung carcinogenesis and clinical implications.

Acknowledgments

We are grateful to Professor K. Inai at the Department of Pathology and Professor N. Kohno at the Department of Molecular and Internal Medicine, Hiroshima University, for providing sample tissues. We also thank Ms. I. Fukuba, Ms. M. Wada, Ms. C. Oda, and Ms. H. Tagawa in our departments for their technical support. Part of this work was carried out at the Department of Molecular and Internal Medicine and the Analysis Center of Life Science, Hiroshima University. This study was partly supported by Grants-in-Aid for Scientific Research from the Ministry of Education, Culture, Science, Sports and Technology of Japan.

References

1. Clarke MF, Dick JE, Dirks PB, Eaves CJ, Jamieson CH, Jones DL, Visvader J, Weissman IL and Wahl GM: Cancer stem cells - perspectives on current status and future directions: AACR Workshop on cancer stem cells. Cancer Res 66: 9339-9344, 2006.
2. Eramo A, Lotti F, Sette G, Pilozzi E, Biffoni M, Di Virgilio A, Conticello C, Ruco L, Peschle C and De Maria R: Identification and expansion of the tumorigenic lung cancer stem cell population. Cell Death Differ 15: 504-514, 2008.
3. Mizrak D, Brittan M and Alison MR: CD133: molecule of the moment. J Pathol 214: 3-9, 2008.
4. Hirschmann-Jax C, Foster AE, Wulf GG, Nuchtern JG, Jax TW, Gobel U, Goodell MA and Brenner MK: A distinct 'side population' of cells with high drug efflux capacity in human tumor cells. Proc Natl Acad Sci USA 101: 14228-14233, 2004.
5. Jiang F, Qiu Q, Khanna A, Todd NW, Deepak J, Xing L, Wang H, Liu Z, Su Y, Stass SA and Katz RL: Aldehyde dehydrogenase 1 is a tumor stem cell-associated marker in lung cancer. Mol Cancer Res 7: 330-338, 2009.
6. Meng X, Li M, Wang X, Wang Y and Ma D: Both $CD133^+$ and $CD133^-$ subpopulations of A549 and H446 cells contain cancer-initiating cells. Cancer Sci 100: 1040-1046, 2009.

7. Lobo NA, Shimono Y, Qian D and Clarke MF: The biology of cancer stem cells. Annu Rev Cell Dev Biol 23: 675-699, 2007.
8. Hiyama E and Hiyama K: Telomere and telomerase in stem cells. Br J Cancer 96: 1020-1024, 2007.
9. Hiyama K, Hiyama E, Tanimoto K and Nishiyama M: Role of telomeres and telomerase in cancer. In: Telomeres and Telomerase in Cancer. Hiyama K (ed.). Humana Press, Springer, New York, NY, pp171-180, 2009.
10. Shapiro GI, Edwards CD, Ewen ME and Rollins BJ: $p16^{INK4A}$ participates in a G1 arrest checkpoint in response to DNA damage. Mol Cell Biol 18: 378-387, 1998.
11. Shay JW and Wright WE: Senescence and immortalization: role of telomeres and telomerase. Carcinogenesis 26: 867-874, 2005.
12. Arifin M, Hiyama K, Tanimoto K, Wiyono WH, Hiyama E and Nishiyama M: EGFR activating aberration occurs independently of other genetic aberrations or telomerase activation in adenocarcinoma of the lung. Oncol Rep 17: 1405-1411, 2007.
13. Sobin LH, Hermanek P and Hutter RV: TNM classification of malignant tumors. A comparison between the new (1987) and the old editions. Cancer 61: 2310-2314, 1988.
14. Hiyama K, Hiyama E, Ishioka S, Yamakido M, Inai K, Gazdar AF, Piatyszek MA and Shay JW: Telomerase activity in small-cell and non-small-cell lung cancers. J Natl Cancer Inst 87: 895-902, 1995.
15. Hiyama K, Ishioka S, Shirotani Y, Inai K, Hiyama E, Murakami I, Isobe T, Inamizu T and Yamakido M: Alterations in telomeric repeat length in lung cancer are associated with loss of heterozygosity in p53 and Rb. Oncogene 10: 937-944, 1995.
16. Mendoza C, Sato H, Hiyama K, Ishioka S, Isobe T, Maeda H, Hiyama E, Inai K and Yamakido M: Allelotype and loss of heterozygosity around the L-myc gene locus in primary lung cancers. Lung Cancer 28: 117-125, 2000.
17. Tanaka T, Tanimoto K, Otani K, Satoh K, Ohtaki M, Yoshida K, Toge T, Yahata H, Tanaka S, Chayama K, Okazaki Y, Hayashizaki Y, Hiyama K and Nishiyama M: Concise prediction models of anticancer efficacy of 8 drugs using expression data from 12 selected genes. Int J Cancer 111: 617-626, 2004.
18. Hiyama K, Tanimoto K, Nishimura Y, Tsugane M, Fukuba I, Sotomaru Y, Hiyama E and Nishiyama M: Exploration of the genes responsible for unlimited proliferation of immortalized lung fibroblasts. Exp Lung Res 34: 373-390, 2008.
19. Herman JG, Graff JR, Myohanen S, Nelkin BD and Baylin SB: Methylation-specific PCR: a novel PCR assay for methylation status of CpG islands. Proc Natl Acad Sci USA 93: 9821-9826, 1996.
20. Hiyama K, Hiyama E and Shay JW: Telomeres and telomerase in humans. In: Telomeres and Telomerase in Cancer. Hiyama K (ed.). Humana Press, Springer, New York, NY, pp3-21, 2009.
21. Hiyama E, Hiyama K, Yokoyama T and Shay JW: Immunohistochemical detection of telomerase (hTERT) protein in human cancer tissues and a subset of cells in normal tissues. Neoplasia 3: 17-26, 2001.
22. Kumazaki T, Hiyama K, Takahashi T, Omatsu H, Tanimoto K, Noguchi T, Hiyama E, Mitsui Y and Nishiyama M: Differential gene expressions during immortalization of normal human fibroblasts and endothelial cells transfected with human telomerase reverse transcriptase gene. Int J Oncol 24: 1435-1442, 2004.
23. Miyazu YM, Miyazawa T, Hiyama K, Kurimoto N, Iwamoto Y, Matsuura H, Kanoh K, Kohno N, Nishiyama M and Hiyama E: Telomerase expression in non-cancerous bronchial epithelia is a possible marker of early development of lung cancer. Cancer Res 65: 9623-9627, 2005.
24. Kraunz KS, Nelson HH, Lemos M, Godleski JJ, Wiencke JK and Kelsey KT: Homozygous deletion of $p16^{INK4a}$ and tobacco carcinogen exposure in nonsmall cell lung cancer. Int J Cancer 118: 1364-1369, 2006.
25. Yokota J and Kohno T: Molecular footprints of human lung cancer progression. Cancer Sci 95: 197-204, 2004.
26. Heppner GH: Tumor heterogeneity. Cancer Res 44: 2259-2265, 1984.
27. Lou H and Dean M: Targeted therapy for cancer stem cells: the patched pathway and ABC transporters. Oncogene 26: 1357-1360, 2007.

Cancer Science
The official journal of the Japanese Cancer Association JCA

Human Arm protein lost in epithelial cancers, on chromosome X 1 (*ALEX1*) gene is transcriptionally regulated by CREB and Wnt/β-catenin signaling

Hiroyoshi Iseki,[1,3] Akihiko Takeda,[1,3,6,7] Toshiwo Andoh,[2,3] Norio Takahashi,[3] Igor V. Kurochkin,[4] Aliaksandr Yarmishyn,[4] Hideaki Shimada,[5,9] Yasushi Okazaki[2,8] and Isamu Koyama[1,3,8]

[1]Department of Digestive Surgery, [2]Division of Functional Genomics and Systems Medicine, and [3]Project Research Division, Research Center for Genomic Medicine, Saitama Medical University, Saitama, Japan; [4]Genome and Gene Expression Data Analysis Division, Bioinformatics Institute, Matrix, Singapore; [5]Department of Digestive Surgery, Chiba Cancer Center, Chiba, Japan; [6]Department of Digestive Surgery, International University of Health and Welfare Hospital, Tochigi, Japan

(Received September 15, 2009/Revised January 29, 2010/Accepted February 3, 2010/Accepted manuscript online March 24, 2010/Article first published online April 20, 2010)

The aberrant activation of Wnt signaling is a key process in colorectal tumorigenesis. Canonical Wnt signaling controls transcription of target genes via β-catenin and T-cell factor/lymphoid enhancer factor family transcription factor complex. Arm protein lost in epithelial cancers, on chromosome X 1 (*ALEX1*) is a novel member of the Armadillo family which has two Armadillo repeats as opposed to more than six repeats in the classical Armadillo family members. Here we examine *cis*-regulatory elements and *trans*-acting factors involved in the transcriptional regulation of the *ALEX1* gene. Site-directed mutations of a cyclic AMP response element (CRE) and an E-box impaired the basal activity of human *ALEX1* promoter in colorectal and pancreatic cancer cell lines. Moreover, overexpression of CRE-binding protein (CREB) increased the *ALEX1* promoter activity in these cell lines, whereas knockdown of *CREB* expression decreased the expression level of *ALEX1* mRNA. Interestingly, luciferase reporter analysis and quantitative real-time RT-PCR demonstrated that the *ALEX1* promoter was up-regulated in a CRE-dependent manner by continuous activation of Wnt/β-catenin signaling induced by a glycogen synthase kinase-3 inhibitor and overexpression of β-catenin. These results indicate that the CRE and E-box sites are essential *cis*-regulatory elements for *ALEX1* promoter activity, and *ALEX1* expression is regulated by CREB and Wntk/β-catenin signaling. (*Cancer Sci* 2010; 101: 1361–1366)

Wnt signaling is important for embryonic development, stem cell maintenance, and tumorigenesis.[1,2] Two Armadillo (Arm) family members, β-catenin and adenomatous polyposis coli (APC), are essential components of the Wnt signaling pathway. β-Catenin is mainly localized to the plasma membrane in normal colon mucosa, whereas the cytoplasmic β-catenin is phosphorylated by the degradation complex composed of casein kinase I, glycogen synthase kinase-3β (GSK-3β), APC, and AXIN, and subsequently degraded by the ubiquitin–proteasome pathway. In over 80% of colorectal cancers, β-catenin aberrantly accumulates in the cytoplasmic and nuclear regions due to inactivating mutations in APC, forming a complex with the T-cell factor/lymphoid enhancer factor (TCF/LEF) family of transcription factors, leading to activation of the Wnt signaling pathway.[3,4] To elucidate the role of the Wnt signaling in tumor development and stem cell maintenance, numerous candidate target genes of the β-catenin/TCF have been identified.[5–7]

The cyclic AMP response element (*CRE*)-binding protein/activating transcription factor (*CREB/ATF*) belongs to the basic region/leucine zipper transcription factor family.[8] Traditionally, it has been believed that CREB dimers bind to CRE sites under basal conditions, but they are inactive; and that activation of CREB is mediated by phosphorylation at a specific serine residue. This phosphorylation promotes the association of CREB with the transcriptional co-activator CREB-binding protein and its paralogue p300, leading to activation of its target genes through histone modification and recruitment of an active transcription complex.[8] It is noteworthy that CREB synergistically or predominantly activates some of its target genes through β-catenin via CRE sites.[9–11]

Arm protein lost in epithelial cancers, on chromosome X (*ALEX*; also known as Armadillo repeat containing, X-linked [*ARMCX*]) is a novel member of the Arm family which has one or two Arm repeats as opposed to more than six repeats in the classical Arm family members.[12] The *ALEX* family, consisting of at least three variants (*ALEX1*, *ALEX2*, and *ALEX3*), is closely localized on chromosome Xq21.33–q22.2.[12] Human *ALEX1* is composed of four exons with the coding region residing entirely in a single exon and encodes a predicted protein of 453 amino acids which is highly conserved between humans and mice (95% amino acid similarity).[13] *ALEX1* mRNA is widely expressed in human tissues but is dramatically reduced or even undetectable in several human carcinoma cell lines and tissues, suggesting that ALEX1 may play a role as a tumor suppressor.[12] However, the regulatory mechanism of the *ALEX1* gene in normal and cancer cells remains largely unknown. Here we examined the transcriptional regulation of the *ALEX1* gene in human cancer cell lines and found that *ALEX1* expression is regulated by CREB and Wnt/β-catenin signaling.

Materials and Methods

Cells and culture conditions. Human colon cancer cell lines HCT116 and SW480 were obtained from DS Pharma Biomedical (Osaka, Japan) and the Cell Resource Center for Biomedical Research, Tohoku University (Sendai, Japan), respectively. Human pancreatic cancer cell line PANC-1 was provided by the RIKEN Cell Bank (Tsukuba, Japan). HCT116 and SW480 cells were cultured in DMEM (Invitrogen, Tokyo, Japan) and PANC-1 cells were cultured in RPMI-1640 (Invitrogen) supplemented with 10% heat-inactivated FBS (Invitrogen) in a 5% CO_2 atmosphere at 37°C.

Plasmid constructs and transfection. The putative promoter region of the human *ALEX1* gene from −1933 to +487 was amplified by PCR and subcloned into the pCR-Blunt II-TOPO

[7]To whom correspondence should be addressed. E-mail: aktake@iuhw.ac.jp
[8]These authors equally contributed to this project in financial support.
[9]Present address: Department of Surgery, School of Medicine, Toho University, 6-11-1, Omorinishi, Ota-ku, Tokyo 143-8541, Japan.

doi: 10.1111/j.1349-7006.2010.01541.x

plasmid (Invitrogen). An approximately 2400-bp DNA fragment containing the *ALEX1* promoter sequence was inserted into the *Eco*RV and *Hin*dIII site of the pGL4.10 plasmid (Promega, Tokyo, Japan). The luciferase reporter plasmids driven by deleted mutant types of *ALEX1* promoter were generated by the same PCR-based method. Point mutations at potential TCF/LEF-binding element (TBE(s)), CRE, and E-box sites were introduced by PCR-based site-directed mutagenesis with PrimeSTAR polymerase (Takara Bio, Shiga, Japan).

Full-length open reading frames for human *ALEX1* and *CTNNB1* genes (accession nos NM_016608 and NM_001904, respectively) were amplified by PCR and inserted into the *Xho*I site of pCAGIPuro plasmid (kindly provided by Dr. H. Niwa, RIKEN), designated as pCAGIPuro/ALEX1 and pCAGIPuro/β-catenin, respectively. The plasmid containing the complete sequence of human *ALEX1* gene and the cDNA derived from HCT116 cells which expresses both wild-type and Ser^{45}-deleted β-catenin were used as templates for the amplification of *ALEX1* and *CTNNB1* genes, respectively.[12] The pCAGIPuro/EGFP plasmid (kindly provided by Dr. H. Niwa, RIKEN) encoding enhanced green fluorescence protein (EGFP) was used as a control.

Human *TCF4* (also known as *TCF7L2*), *ΔN-TCF4*, and *CREB* (*CREBΔ* isoform; accession no. NM 004379) genes were amplified by PCR and inserted into the *Eco*RI site of pCAGIPuro plasmid. Two dominant-negative mutants of the *CREBΔ* gene, $CREB^{R287L}$ (KCREB) and $CREB^{S119A}$ (CREBM1 and mCREB) in which Arg^{287} and Ser^{119} is converted to Leu and Ala, respectively, were generated by PCR-based site-directed mutagenesis.

Plasmid transfections were performed by Lipofectamine 2000 or Lipofectamine LTX (Invitrogen) according to the manufacturer's instructions. Primer sequences used for cloning and mutagenesis are available in Table S1 (Supporting information).

Luciferase reporter assay. The luciferase reporter assay was performed using the Dual-Glo Luciferase Assay System (Promega) according to the manufacturer's instructions. A total of 5000 cells were plated in a 96-well plate. After overnight culture, cells were transfected with 100 ng of the expression plasmid of Firefly reporter gene driven by human *ALEX1* promoter and 50 ng of Renilla luciferase control plasmid (pGL4.74; Promega) using Lipofectamine LTX and cultured for 48 h. TOPflash and FOPflash reporter plasmids (Millipore, Tokyo, Japan), which contain six wild-type and six mutated TBE sites, respectively, were used to evaluate β-catenin/TCF-dependent transcriptional activity. To activate Wnt/β-catenin signaling, cells were treated for 48 h with 6-bromoindirubin-3′-oxime (BIO) (Merck, Tokyo, Japan), at a final concentration of 5 μM, 4 h post transfection. As a control, the cells were treated with deionized distilled water and 5 μM 1-mehyl-6-bromoindirubin-3′-oxime (MeBIO) (Merck), respectively. Firefly and Renilla luciferases were measured by using the 1420 Multilabel Counter ARVO MX. The experiment was performed in triplicate and repeated at least three times.

Quantitative real-time RT-PCR. Total RNA was extracted by RNeasy mini kit (Qiagen, Tokyo, Japan) according to the manufacturer's instructions. First-strand cDNA was synthesized from 1 μg of total RNA using Transcriptor Reverse Transcriptase (Roche Diagnostics, Tokyo, Japan) in a total volume of 20-μL reaction mixtures. Quantitative real-time RT-PCR was performed using the Power SYBR Green PCR Master Mix (Applied Biosystems, Tokyo, Japan) and the MX3000P Real-time PCR System (Stratagene, La Jolla, CA, USA) according to the manufacturers' instructions. Primer sequences are available in Table S1 (Supporting information).

siRNA transfection. PANC-1 cells were transfected with the ON-TARGETplus Non-Targeting Control siRNA or siRNAs targeting CREB using DharmaFECT1 siRNA Transfection Reagent (Thermo Fisher Scientific, Lafayette, CO, USA), and cultured for 48 h. Quantitative real-time RT-PCR was performed using the Rotor-Gene SYBR Green PCR kit (Qiagen) and the Rotor-Gene Q PCR system (Qiagen). The following two ON-TARGETplus siRNAs targeting CREB were used: siRNA1, GAGAGAGGUCCGUCUAAUG; and siRNA2, GCCCAGCCAUCAGUUAUUC.

Chromatin immunoprecipitation (ChIP). ChIP assay was carried out in accordance with a previous report with several modification.[10] Immunoprecipitation was carried out with Dynabeads Protein G (Invitrogen) and polyclonal anti-CREB antibody (#9197; Cell Singling Technology, Danvers, MA, USA). The primer pair used to amplify *ALEX1* and cyclin D1 promoter sequences containing the putative CRE, and *ALEX1* 3′-distal region sequence were as follows: *ALEX1* promoter, 5′-GCTGCTGATGGGAGTGGTA-3′ and 5′-CGGACCAAACGAAGACTAGG-3′; cyclin D1 promoter, 5′-CTCCCGCTCCCATTCTCT-3′ and 5′-ACTCTGCTGCTCGCTGCTAC-3′; and *ALEX1* 3′-distal, 5′-ATGTGCAGCATGAGTCCAAG-3′ and 5′-ATTCCCATGGCCACCAGTA-3′.

Indirect immunofluorescence. The cells were washed in PBS, fixed in 100% methanol at −20°C for 5 min and in 4% paraformaldehyde in PBS at room temperature for 30 min, and permeabilized with 0.2% Triton X-100 in PBS at room temperature for 15 min. Permeabilized cells were washed three times with PBS, treated with 3% bovine serum albumin in PBS for 30 min, followed by incubation with antihuman β-catenin antibody at 1:250 dilution at room temperature for 1 h. After washing three times in PBS, the cells were incubated with Rhodamine-conjugated antimouse IgG antibody (Chemicon) at 1:100 in PBS at room temperature for 1 h. Finally, the cells were mounted in Vectashield Mounting Medium with DAPI (4′,6′-diamidino-2-phenylindole; Vector Laboratories, Burlingame, CA, USA). The images were obtained using a Axiovert 200M fluorescent microscope (Carl Zeiss MicroImaging, Tokyo, Japan).

Statistical analysis. Statistics were performed using the Mann–Whitney *U*-test for the expression analysis and luciferase reporter assay. A *P*-value less than 0.05 was considered to be statistically significant.

Nucleotide sequence accession numbers. The sequences of human *TCF4* gene and human *ALEX1* promoter cloned in this study have been deposited in the DDBJ/EMBL/GenBank databases under accession numbers AB440195 and AB440194, respectively.

Results

CREB regulates human *ALEX1* promoter activity. To identify candidates for *cis*-regulatory elements involved in the regulation of *ALEX1* gene expression, we carried out a computational search for transcription factor binding sites, and found a CRE-B/ATF binding site, CRE, and a basic helix-loop-helix transcription factors-binding site, E-box, at the proximal region of the transcription start site of human *ALEX1* gene (Fig. 1a), which are highly conserved between humans and mice. In addition, six consensus TCF/LEF-binding element (TBE) sites (site nos 8, 9, 10, 11, 12, and 13) and seven imperfect TBE sites (site nos 1, 2, 3, 4, 5, 6, and 7) are located in the upstream and genomic regions of human *ALEX1* gene, respectively (Fig. 1a). Luciferase reporter analysis showed that human *ALEX1* promoter (−1933 to +487), which included a CRE, an E-box, and eight TBE sites, was active in HCT116, SW480, and PANC-1 cells. The site-directed mutations of each CRE and E-box dramatically impaired the luciferase activities in HCT116, SW480, and PANC-1 cells, whereas the mutations of eight TBE sites slightly up-regulated the *ALEX1* promoter activity (Fig. 1b). In addition, co-transfection with a wild-type CREB expression vector induced approximately 4.3-, 2.0-, and 2.1-fold increase in

doi: 10.1111/j.1349-7006.2010.01541.x

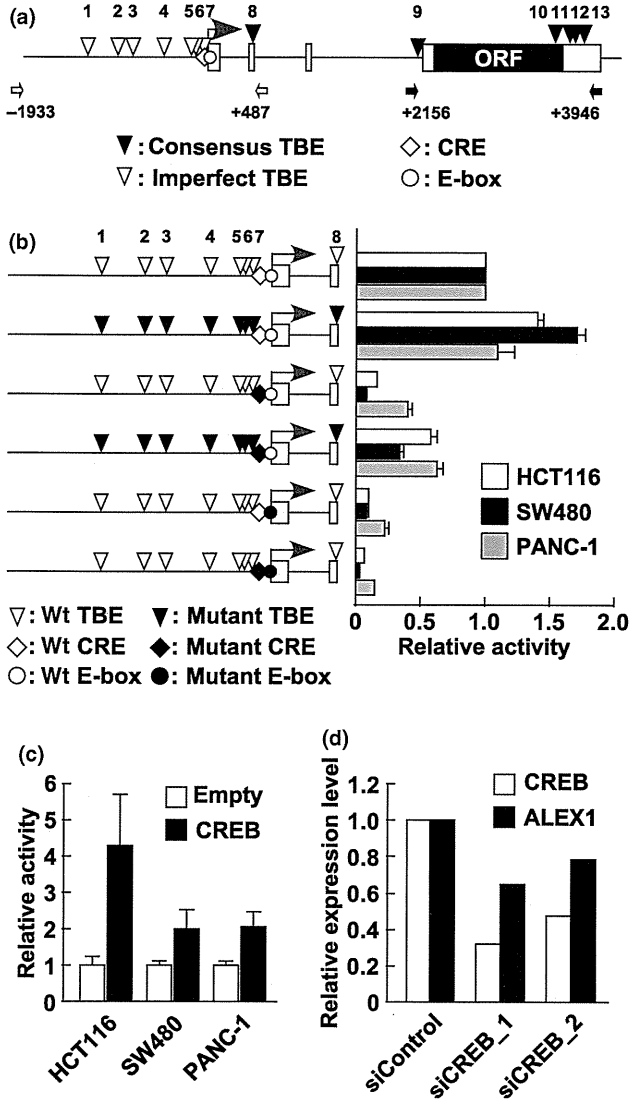

Fig. 1. The cyclic AMP response element (CRE) site and CRE-binding protein (CREB) are involved in human Arm protein lost in epithelial cancers, on chromosome X 1 (*ALEX1*) regulation. (a) A schematic representation of the genomic structure of the *ALEX1* gene on human chromosome X. Open and filled boxes represent the exons of the *ALEX1* gene and the ORF encoding the ALEX1 protein, respectively. The bent arrow indicates the transcription start site of the *ALEX1* gene. The positions of consensus (CTTTGA/TA/T and A/TA/TCAAAG) and imperfect TCF/LEF-binding element (TBE)s are indicated by filled and open reverse triangles, respectively, and numbered. An open diamond and circle represent the putative CRE (TGACGTG) and E-box (CACGTG) site, respectively. The open and closed arrows indicate the primers used for promoter and intron 3-exon 4 regions of the *ALEX1* gene, respectively. (b) In the left diagram, open reverse triangles represent wild-type TBE sites, and filled reverse triangles represent mutated TBE sites. Open and filled diamonds represent the wild-type and mutant type of CRE, respectively. Open and filled circles represent the wild-type and mutant type of E-box, respectively. The right bar graph represents the relative luciferase activities in HCT116, SW480, and PANC-1 cells transfected with the reporter plasmid driven by wild-type and a series of site-directed mutant type of the *ALEX1* promoter. Error bars indicate the SD. (c) Luciferase reporter assay of HCT116, SW480, and PANC-1 cells co-transfected with wild-type *ALEX1* promoter-driven reporter plasmid and the expression plasmid of the indicated genes. Error bars indicate the SD. (d) Quantitative real-time RT-PCR analysis of endogenous *CREB* and *ALEX1* mRNA expression in PANC-1 cells transfected with control siRNA and siRNAs targeting CREB. Relative expression level of *CREB* and *ALEX1* mRNA for each sample was normalized against the expression level of *GAPDH* mRNA. The average of two independent experiments is shown.

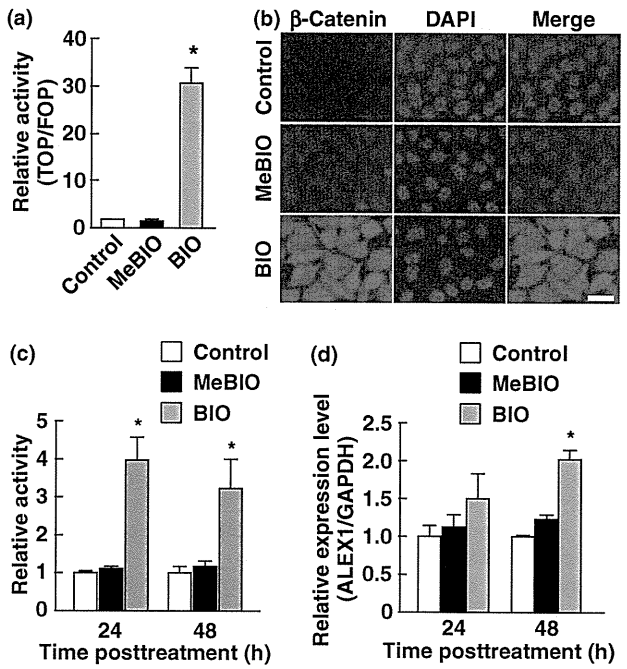

Fig. 2. Glycogen synthase kinase-3 (GSK-3) inhibitor induces human Arm protein lost in epithelial cancers, on chromosome X 1 (*ALEX1*) expression. Luciferase reporter assay of PANC-1 cells treated with/without a GSK-3 inhibitor, 6-bromoindirubin-3′-oxime (BIO), or an inactive analog of BIO, 1-mehyl-6-bromoindirubin-3′-oxime (MeBIO). The bar graph represents the mean ratios between the luciferase activities from TOPflash and FOPflash reporter (TOP/FOP ratio) (a), and relative activities driven by wild-type *ALEX1* promoter (c). (b) Indirect immunofluorescense analysis for β-catenin with PANC-1 cells treated with control solvent, MeBIO, and BIO. Nucleus was stained with DAPI. (d) Quantitative real-time RT-PCR analysis of endogenous *ALEX1* mRNA expressed in PANC-1 cells treated with BIO or MeBIO for 24 and 48 h. Relative expression level of *ALEX1* mRNA for each sample was normalized against the expression level of *GAPDH* mRNA. Error bars indicate the SD. $*P < 0.05$ compared to control and MeBIO-treated cells.

ALEX1 promoter activities in HCT116, SW480, and PANC-1 cells, respectively (Fig. 1c), whereas knockdown of *CREB* expression using two specific siRNAs decreased the *ALEX1* mRNA level in PANC-1 cells (Fig. 1d). These data indicate that both the CRE and E-box sites are essential *cis*-regulatory elements for basal promoter activity of the *ALEX1* gene, and CREB up-regulates the *ALEX1* promoter activity.

Continuous activation of β-catenin up-regulates *ALEX1* expression. The consensus TBE sequence recognized by the β-catenin/TCF complex locates in the proximal promoter regions of several known target genes of canonical Wnt signaling[6,7,14]. To determine whether *ALEX1* gene expression is regulated by Wnt/β-catenin signaling, we examined the expression level and promoter activity of the *ALEX1* gene in GSK-3 inhibitor-treated PANC-1 cells. PANC-1 cells exhibited low levels of β-catenin expression and β-catenin/TCF transcriptional activity (Figs 2a, 3a), and detectable level of endogenous *ALEX1* mRNA by RT-PCR. Activation of the β-catenin/TCF target promoter (TOPflash) and cytoplasmic and nuclear accumulation of β-catenin were markedly induced by GSK-3 inhibitor BIO, but not by MeBIO (a kinase-inactive analog of BIO) (Fig. 2a,b). The luciferase activity of *ALEX1* promoter-driven reporter plasmid was also increased in BIO-treated PANC-1 cells 24 h and 48 h post treatment in comparison to that in solvent-treated control and MeBIO-treated PANC-1 cells (Fig. 2c). In addition, quantitative real-time RT-PCR revealed an increase of endogenous *ALEX1*

mRNA by BIO-treatment (Fig. 2d). Lithium chloride, which is known to function as a GSK-3 inhibitor, also induced an increase of *ALEX1* mRNA (data not shown). These results demonstrate that activation of Wnt/β-catenin signaling by GSK-3 inhibition up-regulates the promoter activity and gene expression of *ALEX1*.

Furthermore, to validate whether cytoplasmic and nuclear accumulation of β-catenin using genetic mutant also activates the *ALEX1* gene, we generated the stable clones of PANC-1 cells expressing the degradation-resistant β-catenin mutant with a deletion of Ser^{45}, which is a phosphorylation site for GSK-3β priming, designated as PANC-1/β-catenin-ΔS45. As a result, two PANC-1/β-catenin-ΔS45 clones showed higher expression levels of β-catenin protein and activation of the target promoter of β-catenin/TCF compared with those in the control PANC-1/empty and PANC-1/EGFP clones (Fig. 3a,b). Quantitative real-time RT-PCR and luciferase reporter analysis revealed significant elevations of endogenous mRNA expression and promoter activity of *ALEX1* in the PANC-1/β-catenin-ΔS45 clones (Fig. 3c,d), indicating that *ALEX1* gene is regulated by Wnt/β-catenin signaling.

Regulation of *ALEX1* gene expression by β-catenin is CRE dependent. Since comparable induction by BIO was obtained using the *ALEX1* promoter-driven reporter plasmids with/without intron 3-exon 4 region containing five TBE sites (+2156 to +3946; Fig. 4a), we used the *ALEX1* promoter-driven reporter plasmid without intron 3-exon 4 region to elucidate a regulatory region required for β-catenin stimulation. A series of 5′ deletions and site-directed mutations of TBE sites exhibited little impairment in response to Wnt/β-catenin signaling induced by BIO (Fig. 4b). Furthermore, the activation of the *ALEX1* promoter was suppressed by the overexpression of the N-terminal deletion mutant of TCF4 (ΔN-TCF4) known to block the transcriptional activity of β-catenin due to lack of the β-catenin binding domain (Fig. 4c). Previous studies have reported that transcription factors, including CREB, are capable of recruiting β-catenin;[10,15–17] thus, we evaluated the effect of the CRE site on β-catenin-mediated transactivation of the *ALEX1* promoter by luciferase reporter assay. Interestingly, the mutation of the CRE site resulted in almost complete loss of induction by BIO (Fig. 4b). These data suggest that the CRE site plays an important role in mediating β-catenin-dependent transcriptional activation of the *ALEX1* promoter, whereas the TBE sites play only a minor role although TCF4 may contribute to this activation.

The transcriptional relevance of CREB in regulating the *ALEX1* expression in the PANC-1/empty and the PANC-1/β-catenin-ΔS45 clones was further confirmed by ChIP assay (Fig. 4d). To further investigate whether CREB mediates activation of the *ALEX1* promoter by β-catenin, wild-type CREB and two dominant-negative mutants, $CREB^{R287L}$ and $CREB^{S119A}$, were overexpressed in BIO-treated PANC-1 cells. The luciferase reporter analysis for the *ALEX1* promoter showed that the response to β-catenin was enhanced by the wild-type CREB but was suppressed by a DNA-binding defective mutant $CREB^{R287L}$ (Fig. 4c), indicating that CREB, at least in part, mediates the transcriptional activation of the *ALEX1* gene by Wnt/β-catenin signaling. Surprisingly, a Ser^{119} phosphorylation-defective mutant $CREB^{S119A}$ enhanced the activation of the *ALEX1* promoter by BIO, suggesting that BIO-induced activation of the *ALEX1* promoter is independent of the phosphorylation of CREB at Ser^{119} which is important for transcriptional activation of several CREB target genes.

Discussion

Arm family members exert diverse functions through interactions of their Arm repeat domain with several binding partners.

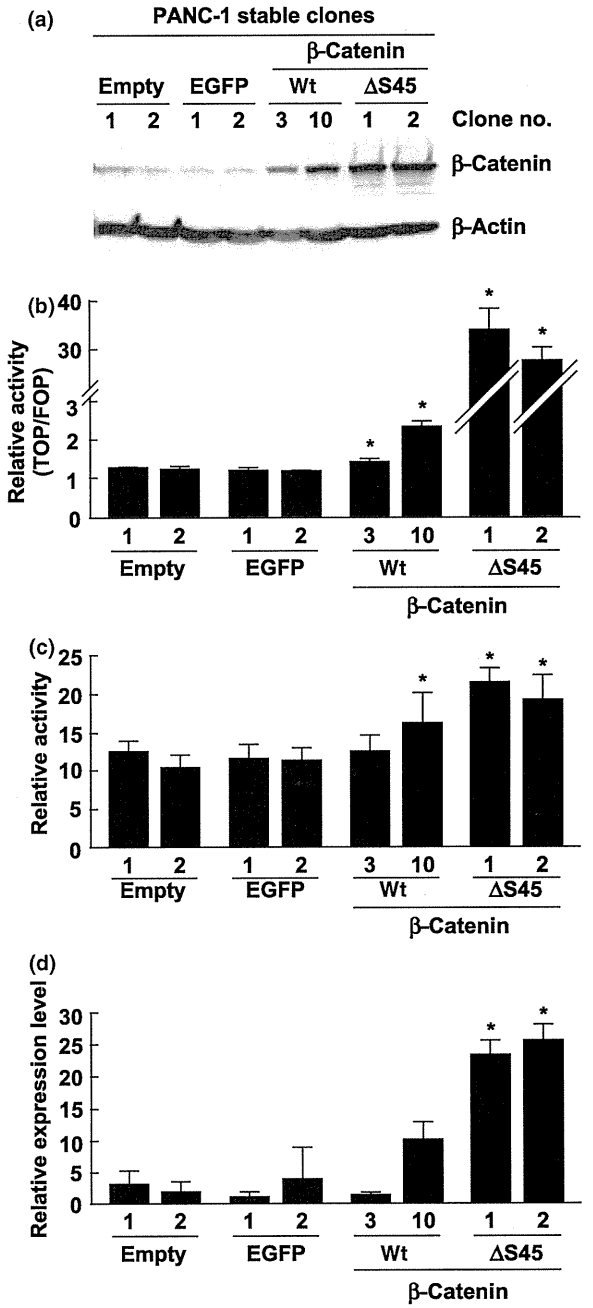

Fig. 3. Overexpression of the constitutive-active mutant type of β-catenin induces human Arm protein lost in epithelial cancers, on chromosome X 1 (*ALEX1*) expression. (a) Western blot analysis for β-catenin was performed with the cell lysate from stably transfected PANC-1/empty, PANC-1/EGFP, PANC-1/β-catenin-wt, and PANC-1/β-catenin-ΔS45 clones. β-Actin protein served as an internal control. (b) Luciferase reporter assay of stably transfected PANC-1 clones transfected with reporter constructs. The bar graph represents the mean ratios between the luciferase activities from TOPflash and FOPflash reporter (TOP/FOP ratio). The error bars represent the SD. $*P < 0.05$ compared to each control clone (empty nos 1 and 2, and EGFP nos 1 and 2). (c) Luciferase reporter assay of each stably transfected PANC-1 clone transfected with wild-type *ALEX1* promoter-driven reporter plasmid. The bar graph represents the relative luciferase activities, and the error bars represent the SD. $*P < 0.05$ compared to each control clone (empty nos 1 and 2, and EGFP nos 1 and 2). (d) Quantitative real-time RT-PCR analysis of endogenous *ALEX1* mRNA of stably transfected PANC-1 clone. The relative level of *ALEX1* mRNA expression for each sample was normalized against the expression level of *GAPDH* mRNA. $*P < 0.05$ compared to each control clone (empty nos 1 and 2, and EGFP nos 1 and 2).

doi: 10.1111/j.1349-7006.2010.01541.x

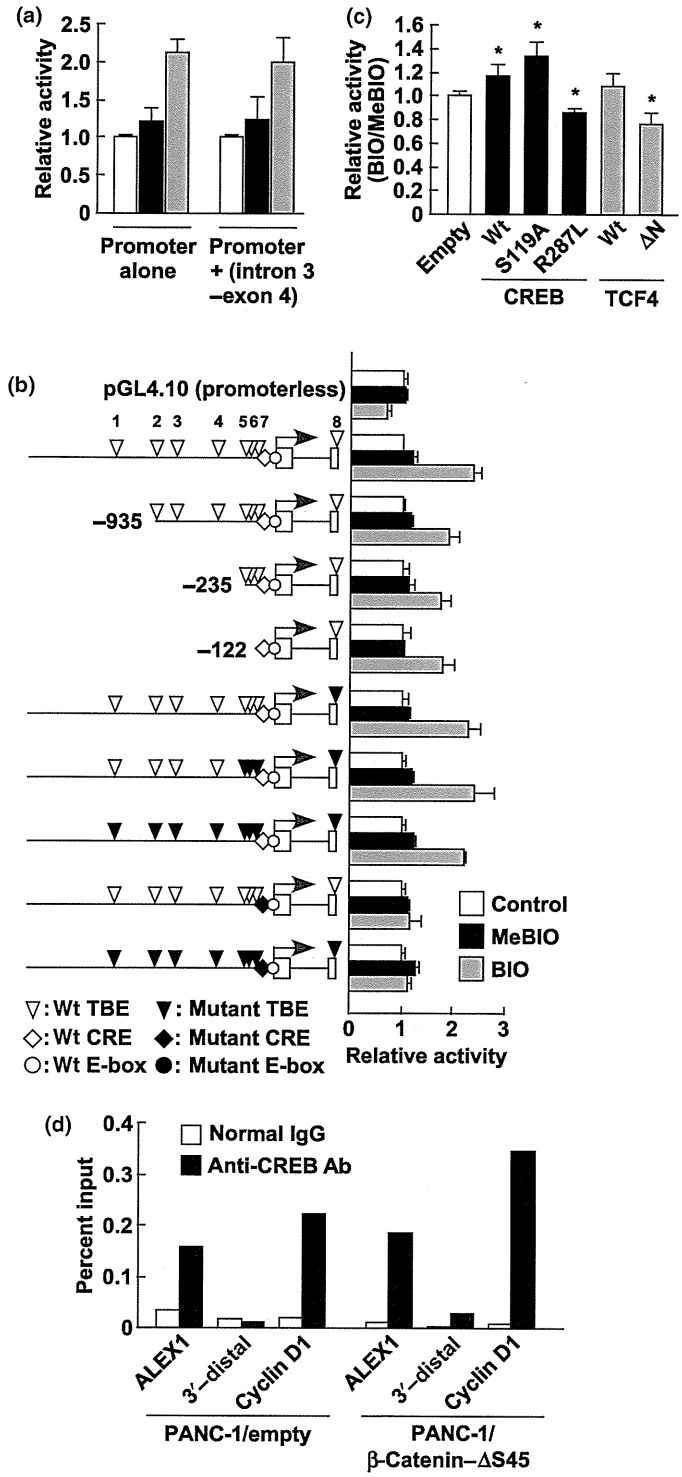

Fig. 4. Cyclic AMP response element (CRE)-site and CRE-binding protein (CREB)-mediated activation of human Arm protein lost in epithelial cancers, on chromosome X1 (*ALEX1*) promoter by the glycogen synthase kinase-3 (GSK-3) inhibitor. (a) Luciferase reporter assay of PANC-1 cells transfected with wild-type *ALEX1* promoter-driven reporter plasmid with/without the intron 3-exon 4 region containing five TBE sites (+2156 to +3946). The bar graph represents the relative luciferase activities. (b) The left diagram is shown as described in the legend for Figure 1(b). The right bar graph represents the relative luciferase activities in control, 1-mehyl-6-bromoindirubin-3′-oxime (MeBIO)-, and 6-bromoindirubin-3′-oxime (BIO)-treated PANC-1 cells transfected with the reporter plasmid driven by wild-type, a series of 5′ deleted type, or a series of the site-directed mutant type of human *ALEX1* promoter. The error bars indicate the SD. (c) Luciferase reporter assay of PANC-1 cells co-transfected with wild-type *ALEX1* promoter-driven reporter plasmid and expression plasmid of the indicated genes. The bar graph represents the mean ratios between the luciferase activities in PANC-1 cells treated with BIO and MeBIO (BIO/MeBIO ratio), and the error bars represent the SD. $*P < 0.05$ compared to control (empty). (d) Chromatin immunoprecipitation followed by quantitative real-time PCR was carried out with normal rabbit IgG or anti-CREB antibody using the PANC-1/empty clone 1 and PANC-1/β-catenin-ΔS45 clone 1. Sequences of cyclin D1 promoter and 3′-distal region of the *ALEX1* gene were used as a positive and negative control for CREB binding, respectively.

ALEX1 and its homologs are not classical members of the Arm family and represent a new family of proteins with less than six Arm repeats. Here we revealed the *cis*-regulatory elements and *trans*-acting factors involved in the transcriptional regulation of the *ALEX1* gene. First, we demonstrated that potential CRE and E-box sites were essential *cis*-regulatory elements for basal transcription of the human *ALEX1* gene. A CRE and an E-box are known to be occupied by the CREB/ATF family and the basic helix-loop-helix family of transcription factors, respectively. Since overexpression and knockdown of CREB altered the *ALEX1* promoter activity, CREB may play an important role in regulating *ALEX1* gene expression. In addition, ChIP assay also supported the role of CREB in transcriptional activation of the *ALEX1* gene via binding to the proximal promoter region including the CRE site. However, the response of the *ALEX1* promoter to CREB induction was not diminished by the CRE mutation (Fig. S1, Supporting information). Several genes have been found to be regulated by CREB via multiple CRE sites, and point mutations in one CRE site alone are not enough to impair its promoter activity. Luciferase reporter analysis using a series of 5′ deletions of the *ALEX1* promoter-driven vector suggests that at least the proximal promoter region (−122 to +487) contains a CREB response sequence (Fig. S1, Supporting information). In the case of the *ALEX1* gene, CREB might regulate via multiple CRE sites which are uncovered in this paper. Further studies are needed to identify transcription factors regulating *ALEX1* gene expression through the E-box site. Second, we showed that Wnt/β-catenin signaling up-regulated *ALEX1* gene expression and transcriptional activation of the *ALEX1* gene by β-catenin mediated by the CRE site. It is believed that β-catenin binds DNA indirectly through the interaction with a member of the TCF/LEF family because β-catenin does not possess a DNA-binding domain.[18] However, a genome-wide analysis of β-catenin occupancy revealed a lack of consensus TBE motif in 16% of target genes,[19] suggesting that β-catenin binds to this group of targets indirectly through a nonconsensus TBE motif or an unrelated factor-binding site. In fact, the transcription factors FOXO, Pit1, and Prop1 recruit β-catenin to their target gene promoters.[15–17] Furthermore, recent studies have provided evidence supporting the importance of CRE sites in Wnt signaling, since interaction with CREB is required for β-catenin to activate the cyclin D1 and cyclooxygenase-2 promoter.[10,20] In this report, a GSK-3 inhibitor and β-catenin up-regulated *ALEX1* gene expression (Figs 2,3). Importantly, BIO-induced activation of the *ALEX1* promoter was little affected by the mutations of TBE sites, but almost completely abolished by the mutation of the CRE site (Fig. 4a). Moreover, overexpression of CREB enhanced BIO-induced *ALEX1* promoter activation (Fig. 4b). Taken together, *ALEX1* is thought to be regulated by Wnt/β-catenin signaling; however, the regulation of *ALEX1* gene expression by β-catenin may be mediated by the CRE but not TBE sites. Third, the CREB-mediated regulation of *ALEX1* gene expression by β-catenin was CREB phosphorylation independent. The $CREB^{R287L}$ mutant, which blocks binding of wild-type CREB to CRE sites through heterodimer formation,[21] was

observed to reduce the response to β-catenin (Fig. 4c). However, the overexpression of the $CREB^{S119A}$ mutant, which underwent a point mutation at a potential phosphorylation site by several kinases such as a cAMP-dependent protein kinase, was observed to accelerate responses to β-catenin at similar levels of induction as those by overexpression of wild-type CREB (Fig. 4c). The phosphorylation of Ser^{119} is essential for the transcriptional activation of CREB, but not for DNA binding.[8] Therefore, the binding of CREB to the CRE sites is considered to be a prerequisite for the transcriptional activation of the *ALEX1* gene by β-catenin, and CREB phosphorylation may be dispensable for this activation.

The dysregulation of the Wnt signaling can contribute to tumor development mainly by activation of target gene expression such as c-*myc* and cyclin D1, whereas Wnt antagonists such as secreted frizzled-related proteins, dickkopf-1, and Wnt inhibitor factor-1 are also up-regulated by Wnt signaling, leading to the negative feedback regulation of Wnt signaling. The present data indicate that *ALEX1* is regulated by Wnt/β-catenin signaling. In addition, overexpression of ALEX1 suppresses the colony formation of colorectal cancer cell lines and is frequently down-regulated in human colorectal cancer (manuscript in preparation). Thus, it is speculated that ALEX1 might act as a negative regulator of cell proliferation promoted by aberrant activation of Wnt/β-catenin signaling.

In summary, the current results indicate that *ALEX1* is a potential target gene of CREB, and Wnt/β-catenin signaling regulates *ALEX1* gene expression. The CRE is important for basal promoter activity and the transcriptional activation of *ALEX1* gene response to β-catenin. This is the first study to investigate the transcriptional regulation of the ALEX family, and these findings may provide new insights into the molecular mechanism underlying the CREB function and Wnt/β-catenin signaling.

Acknowledgments

The authors thank Hitoshi Niwa of the RIKEN Center for Developmental Biology for the generous gift of the pCAGIPuro and pCAGIPuro/EGFP plasmids. The authors also thank members of the Division of Functional Genomics and Systems Medicine for helpful discussion and advice. This work was partly supported by a Grant-in-Aid for Development of New Technology from The Promotion and Mutual Aid Corporation for Private Schools of Japan (2008).

References

1 Reya T, Clevers H. Wnt signalling in stem cells and cancer. *Nature* 2005; **434**: 843–50.
2 Katoh M. WNT signaling pathway and stem cell signaling network. *Clin Cancer Res* 2007; **13**: 4042–5.
3 Goss KH, Groden J. Biology of the adenomatous polyposis coli tumor suppressor. *J Clin Oncol* 2000; **18**: 1967–79.
4 Wong SC, Lo ES, Lee KC, Chan JK, Hsiao WL. Prognostic and diagnostic significance of β-catenin nuclear immunostaining in colorectal cancer. *Clin Cancer Res* 2004; **10**: 1401–8.
5 Shtutman M, Zhurinsky J, Simcha I *et al.* The cyclin D1 gene is a target of the b-catenin/LEF-1 pathway. *Proc Natl Acad Sci USA* 1999; **96**: 5522–7.
6 He TC, Sparks AB, Rago C *et al.* Identification of c-MYC as a target of the APC pathway. *Science* 1998; **281**: 1509–12.
7 Tetsu O, McCormick F. β-Catenin regulates expression of cyclin D1 in colon carcinoma cells. *Nature* 1999; **398**: 422–6.
8 Mayr B, Montminy M. Transcriptional regulation by the phosphorylation-dependent factor CREB. *Nat Rev Mol Cell Biol* 2001; **2**: 599–609.
9 Xu L, Corcoran RB, Welsh JW, Pennica D, Levine AJ. WISP-1 is a Wnt-1- and b-catenin-responsive oncogene. *Genes Dev* 2000; **14**: 585–95.
10 Pradeep A, Sharma C, Sathyanarayana P *et al.* Gastrin-mediated activation of cyclin D1 transcription involves β-catenin and CREB pathways in gastric cancer cells. *Oncogene* 2004; **23**: 3689–99.
11 Giese K, Kingsley C, Kirshner JR, Grosschedl R. Assembly and function of a TCRα enhancer complex is dependent on LEF-1-induced DNA bending and multiple protein-protein interactions. *Genes Dev* 1995; **9**: 995–1008.
12 Kurochkin IV, Yonemitsu N, Funahashi SI, Nomura H. ALEX1, a novel human armadillo repeat protein that is expressed differentially in normal tissues and carcinomas. *Biochem Biophys Res Commun* 2001; **280**: 340–7.
13 Smith CA, McClive PJ, Sinclair AH. Temporal and spatial expression profile of the novel armadillo-related gene, Alex2, during testicular differentiation in the mouse embryo. *Dev Dyn* 2005; **233**: 188–93.
14 Easwaran V, Lee SH, Inge L *et al.* β-Catenin regulates vascular endothelial growth factor expression in colon cancer. *Cancer Res* 2003; **63**: 3145–53.
15 Kioussi C, Briata P, Baek SH *et al.* Identification of a Wnt/Dvl/β-Catenin –> Pitx2 pathway mediating cell-type-specific proliferation during development. *Cell* 2002; **111**: 673–85.
16 Olson LE, Tollkuhn J, Scafoglio C *et al.* Homeodomain-mediated β-catenin-dependent switching events dictate cell-lineage determination. *Cell* 2006; **125**: 593–605.
17 Essers MA, de Vries-Smits LM, Barker N, Polderman PE, Burgering BM, Korswagen HC. Functional interaction between β-catenin and FOXO in oxidative stress signaling. *Science* 2005; **308**: 1181–4.
18 Xu W, Kimelman D. Mechanistic insights from structural studies of β-catenin and its binding partners. *J Cell Sci* 2007; **120**: 3337–44.
19 Yochum GS, McWeeney S, Rajaraman V, Cleland R, Peters S, Goodman RH. Serial analysis of chromatin occupancy identifies β-catenin target genes in colorectal carcinoma cells. *Proc Natl Acad Sci USA* 2007; **104**: 3324–9.
20 Wang H, Wen S, Bunnett NW, Leduc R, Hollenberg MD, MacNaughton WK. Proteinase-activated receptor-2 induces cyclooxygenase-2 expression through β-catenin and cyclic AMP-response element-binding protein. *J Biol Chem* 2008; **283**: 809–15.
21 Shaywitz AJ, Greenberg ME. CREB: a stimulus-induced transcription factor activated by a diverse array of extracellular signals. *Annu Rev Biochem* 1999; **68**: 821–61.

Supporting Information

Additional Supporting Information may be found in the online version of this article:

Table S1. Primer sequences used in this study.

Fig. S1. The proximal regulatory region of the Arm protein lost in epithelial cancers, on chromosome X 1 (*ALEX1*) gene responds to cyclic AMP response element binding protein (CREB) induction. Luciferase reporter assay of PANC-1 cells co-transfected with the reporter plasmid driven by a series of deletion and site-directed mutant types of the ALEX1 promoter, and the CREB expression plasmid or control empty plasmid. Error bars indicate the SD.

doi: 10.1111/j.1349-7006.2010.01541.x

THE JOURNAL OF BIOLOGICAL CHEMISTRY VOL. 285, NO. 20, pp. 15577–15586, May 14, 2010

Dual Roles of Smad Proteins in the Conversion from Myoblasts to Osteoblastic Cells by Bone Morphogenetic Proteins*[S]

Received for publication, May 31, 2009, and in revised form, March 5, 2010 Published, JBC Papers in Press, March 15, 2010, DOI 10.1074/jbc.M109.028019

Junya Nojima[‡§], Kazuhiro Kanomata[‡], Yumi Takada[¶], Toru Fukuda[‡], Shoichiro Kokabu[‡§], Satoshi Ohte[‡], Takatora Takada[¶], Tohru Tsukui[‖], Takamasa S. Yamamoto[**], Hiroki Sasanuma[‡], Katsumi Yoneyama[‡], Naoto Ueno[**], Yasushi Okazaki[‡‡], Ryutaro Kamijo[¶], Tetsuya Yoda[§], and Takenobu Katagiri[‡1]

From the Divisions of [‡]Pathophysiology, [‖]Experimental Animal Laboratory, and [‡‡]Functional Genomics and System Research, Research Center for Genomic Medicine, Saitama Medical University, 1397-1 Yamane, Hidaka-shi, Saitama 350-1241, the [§]Department of Oral and Maxillofacial Surgery, Faculty of Medicine, Saitama Medical University, 38 Moro Hongo, Moroyama-machi, Iruma-gun, Saitama 350-0495, the [¶]Department of Biochemistry, School of Dentistry, Showa University, 1-5-8 Hatanodai, Shinagawa-ku, Tokyo 142-5555, and the [**]Division of Morphogenesis, Department of Developmental Biology, National Institute for Basic Biology, 38 Nishigonaka, Myodaiji, Okazaki, Aichi 444-8585, Japan

Bone morphogenetic proteins (BMPs) induce ectopic bone formation in muscle tissue *in vivo* and convert myoblasts such that they differentiate into osteoblastic cells *in vitro*. We report here that constitutively active Smad1 induced osteoblastic differentiation of C2C12 myoblasts in cooperation with Smad4 or Runx2. In floxed Smad4 mice-derived cells, Smad4 ablation partially suppressed BMP-4-induced osteoblast differentiation. In contrast, the BMP-4-induced inhibition of myogenesis was lost by Smad4 ablation and restored by Smad4 overexpression. A nuclear zinc finger protein, E4F1, was identified as a possible component of the Smad4 complex that suppresses myogenic differentiation in response to BMP signaling. In the presence of Smad4, E4F1 stimulated the expression of *Ids*. Taken together, these findings suggest that the Smad signaling pathway may play a dual role in the BMP-induced conversion of myoblasts to osteoblastic cells.

Bone morphogenetic proteins (BMPs)[2] are members of the transforming growth factor-β (TGF-β) superfamily, which regulates the differentiation, proliferation, and death of various types of cells (1). BMPs were originally found in bone matrix as factors responsible for the induction of ectopic bone formation, in which implantation of demineralized bone matrix into muscle tissue induced new bone tissue containing bone marrow (2, 3). Implantation of individual recombinant BMPs, such as BMP-2, BMP-4, BMP-6, and BMP-7, into muscle tissue induces ectopic bone formation *in vivo* as well (4). This ectopic bone-inducing activity is highly specific to BMPs, because other hormones and cytokines, including TGF-β1 itself, failed to induce ectopic bone formation in muscle tissue *in vivo* (5). Although many factors, such as BMPs, TGF-βs, fibroblast growth factors, and epidermal growth factor, inhibit myogenic maturation of myoblasts *in vitro*, only BMPs convert them so that they differentiate to osteoblastic cells, the bone-forming cells in vertebrates (6–10). Thus, the activity of BMPs in myoblast cultures to induce osteoblastic differentiation appears to reflect the ectopic bone-inducing activity of BMPs *in vivo* (8).

BMP signaling is transduced by two different types of serine/threonine kinase receptors, termed type I and II receptors (1, 11, 12). The BMP-bound type II receptor phosphorylates the type I receptor kinase, and the activated BMP type I receptor in turn phosphorylates downstream substrates such as receptor-regulated Smads (R-Smads), including Smad1, Smad5, and Smad8 and p38 mitogen-activated protein kinase. Phosphorylated R-Smads form heteromeric complexes with Smad4 and translocate into the nucleus to regulate transcription of various target genes, including *Id1*, which encodes a dominant-negative inhibitor of myogenesis (13–15). Recently, a genetic mutation of ALK2, a BMP type I receptor, was identified in patients with fibrodysplasia ossificans progressiva, an autosomal-dominant disorder characterized by heterotopic bone formation in muscle tissue (16). Our findings indicate that this mutant ALK2 is a constitutively activated and hyper-reactive form of the BMP type I receptor and suggest that downstream signaling of activated receptors play an important role in heterotopic bone formation in muscle tissue under certain pathological conditions (17).

Here, we show that a protein in which the carboxyl-terminal serine residues of Smad1 were substituted with aspartic acids, termed Smad1(DVD), functioned as a constitutively activated

* This work was supported in part by Health and Labor Sciences Research Grants for Research on Measures for Intractable Research from the Ministry of Health, Labor and Welfare of Japan (to T. K.), grant-in-aids from Saitama Medical University Internal Grants (to T. F. and T. K.), grant-in-aids from the Ministry of Education, Culture, Sports, Science, and Technology of Japan (to T. F. and T. K.), a grant-in-aid for "Support Project of Strategic Research Center in Private Universities" from the Ministry of Education, Culture, Sports, Science and Technology of Japan to Saitama Medical University Research Center for Genomic Medicine (to T. K.), a grant-in-aid from the Sankyo Foundation of Life Science (to T. K.), a grant-in-aid from the Kawano Masanori Memorial Foundation for Promotion of Pediatrics (to T. K.), a grant-in-aid from the Novo Nordisk Award for Growth and Development (to T. K.), a grant-in-aid from Japan Intractable Diseases Research Foundation (to T. F.), and a grant-in-aid from the Takeda Science Foundation (to T. K.).

[S] The on-line version of this article (available at http://www.jbc.org) contains supplemental Figs. S1–S3.

[1] To whom correspondence should be addressed. Tel.: 81-42-984-0443; Fax: 81-42-984-4651; E-mail: katagiri@saitama-med.ac.jp.

[2] The abbreviations used are: BMP, bone morphogenetic protein; ALP, alkaline phosphatase; BMPR-IA, bone morphogenetic protein receptor type IA; MHC, myosin heavy chain; TGF-β, transforming growth factor-β; ChIP, chromatin immunoprecipitation; NLS, nuclear localization signal; EGFP, enhanced green fluorescent protein; MEF, mouse embryonic fibroblast; RNAi, RNA interference; siRNA, small interfering RNA; R-Smad, receptor-regulated Smad; luc, luciferase.

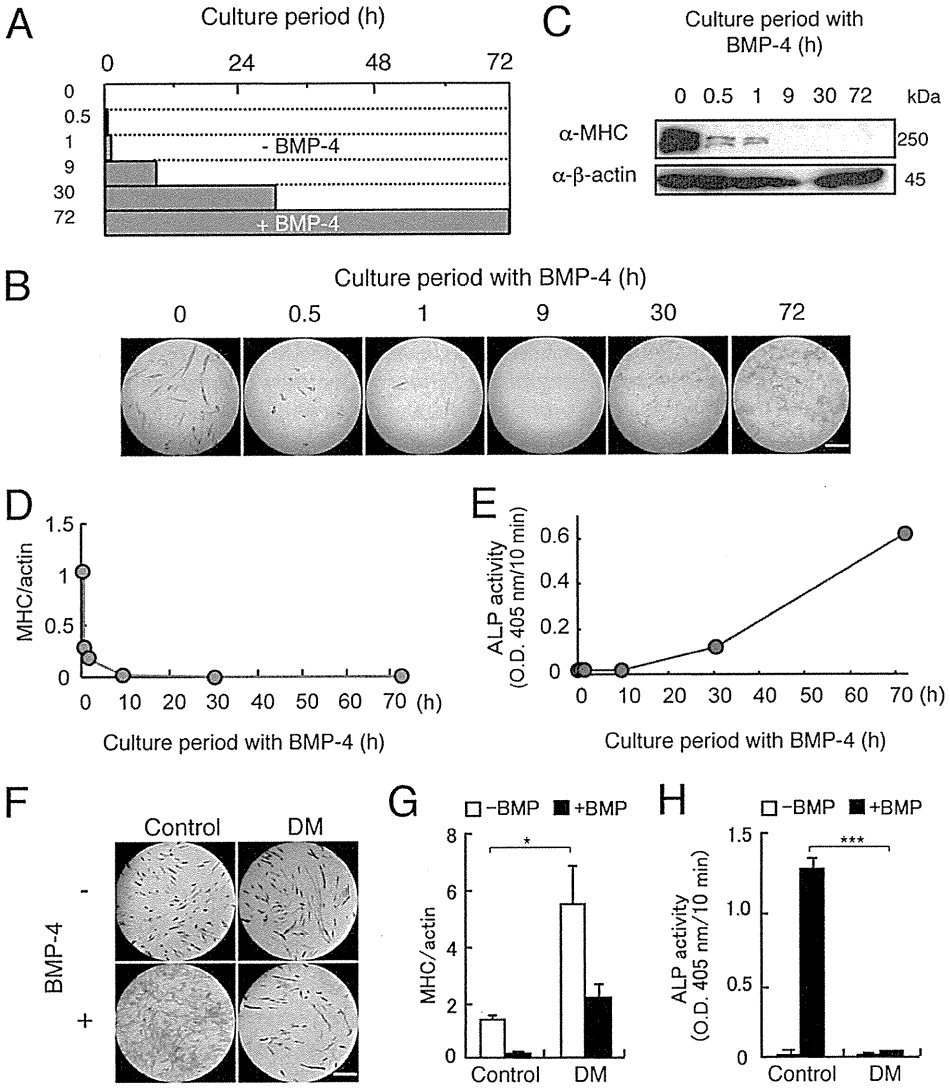

FIGURE 1. **Smad signaling pathway regulates both inhibition of myogenic differentiation and induction of osteoblastic differentiation by BMP-4.** *A* and *B*, examination of the minimal treatment periods required for inhibition of myogenic differentiation and induction of osteoblastic differentiation by BMP-4 in C2C12 myoblasts. *A*, scheme of treatment of C2C12 myoblasts with BMP-4 in a window experiment. C2C12 cells were treated for 0, 0.5, 1, 9, 30, or 72 h with 100 ng/ml of BMP-4 (*closed bars*) and further incubated without BMP-4 (*open bars*) until 72 h before staining. *B*, the cells were doubly stained for ALP and MHC in *blue* and *red*, respectively, at 72 h. *Scale bar*, 200 μm. *C–E*, quantitation of the effects of BMP-4 on myogenic differentiation and osteoblastic differentiation of C2C12 cells. Western blots for MHC (*C* and *D*) and measurement of ALP activity (*E*) were performed on day 3. *F–H*, effects of Dorsomorphin on BMP-induced differentiation in C2C12 cells. C2C12 cells were preincubated for 1 h with 3 μM Dorsomorphin (DM) and 100 ng/ml of BMP-4 was then added. *F*, the cells were doubly stained for ALP and MHC on day 3. *Scale bar*, 400 μm. MHC levels (*G*) and ALP activity (*H*) were measured on day 3. Values are mean ± S.D. ($n = 3$). *, $p < 0.05$; ***, $p < 0.001$.

Smad1. Overexpression of Smad1(DVD) induced osteoblastic differentiation of C2C12 myoblasts, although the inhibition of myogenic differentiation depended principally on nuclear Smad4 rather than R-Smads. E4F1 was identified as a possible component of the Smad4 complex in the suppression of myogenic differentiation by BMP signaling. R-Smads and Smad4 play important roles in the conversion of myogenic cells to osteoblastic cells by BMPs, data were confirmed with the deletion of Smad4 in mouse embryonic fibroblasts (MEFs).

EXPERIMENTAL PROCEDURES

Expression Vectors—Expression vectors for wild-type mouse Smad1, Smad4, and Smad7 were described previously (13). All of the mutations were introduced by a standard PCR technique using Platinum Pfx DNA polymerase (Invitrogen) and their sequences were confirmed in each expression vector. Smad1 mutants were obtained by substitution of Ser-463 and/or Ser-465 of mouse Smad1 with aspartic acid or alanine residues. A nuclear localization signal derived from an SV40 large T antigen, PPKKKRKV, was inserted between an amino-terminal epitope tag and Smad1 or Smad4. NLS-Smad4(ΔMH1) and NLS-Smad4(ΔMH2) were obtained by deleting amino acids 2–138 and 316–552, respectively, from full-length NLS-Smad4. Both mouse wild-type and dominant-negative Runx2 vectors were kindly provided by Dr. Toshihisa Komori (Nagasaki University) (18). Mouse *E4f1* (accession number BC057011) cDNA was obtained by a standard reverse transcription-PCR technique and cloned into pcDEF3 with a FLAG epitope sequence at the 3′ end (19), and E4F1(ΔE3) and the zinc finger mutants (Z1–Z6) were generated by deleting a ubiquitin E3 ligase domain, amino acids 40–84, and substituting two cysteine residues with alanines at positions 195 and 197, 223 and 226, 435 and 438, 519 and 522, and 547 and 550, respectively.

Cell Cultures and Transfections—C2C12 mouse myoblasts, C3H10T1/2 mouse fibroblasts, and COS-7 African green monkey kidney cells were maintained as described (8, 20). The cells were treated with 100 ng/ml of recombinant human BMP-4 (R & D Systems, Inc.) in the presence or absence of chemical inhibitors of mitogen-activated protein kinase, U0126, SB203580, or SP600125 (Merck, Tokyo, Japan) or of the BMP Smad pathway, Dorsomorphin (Calbiochem, San Diego, CA) (20, 21). Lipofectamine 2000 (Invitrogen) was used for plasmid transfections. RNAi Stealth oligonucleotides against murine *Smad1* (MSS275578), *Smad5* (MSS2755978), *Runx2* (MSS202675), *Smad4* (MSS206437), and *E4f1* (MSS274050) and a scrambled negative control oligonucleotide were purchased from Invitrogen. An expression plasmid for *E4f1* microRNA was constructed by subcloning Mmi508063 (Invitrogen) into pcDNA6.2-GW/EmGFP-miR (Invitrogen). MEFs prepared from *Smad4*$^{floxed/floxed}$ mouse embryos at 11.5 days postcoitum were infected with an